Geology and Stratigraphic Correlation of the Murray and Carolyn Shoemaker Formations Across the Glen Torridon Region, Gale Crater, Mars

C M Fedo, A B Bryk, L A Edgar, K A Bennett, V K Fox, W E Dietrich, S G Banham, S. Gupta, K M Stack, R M E Williams, et al.

JGR Planets

RESEARCH ARTICLE
10.1029/2022JE007408

Special Section:
The Curiosity rover's investigation of Glen Torridon and the surrounding area

Key Points:

- Cross-bedded Knockfarril Hill member strata overlie mudstone of the Jura member indicating an environmental change from lake to fluvial
- A geologic map of Glen Torridon (GT) made using lithologically defined stratigraphic units shows that strata dip two degrees or less to the NNW
- Stratigraphic units pass from Vera Rubin ridge into GT indicating that strata continue through a major geomorphic boundary

Correspondence to:
C. M. Fedo,
cfedo@utk.edu

Citation:
Fedo, C. M., Bryk, A. B., Edgar, L. A., Bennett, K. A., Fox, V. K., Dietrich, W. E., et al. (2022). Geology and stratigraphic correlation of the Murray and Carolyn Shoemaker formations across the Glen Torridon region, Gale crater, Mars. *Journal of Geophysical Research: Planets*, *127*, e2022JE007408. https://doi.org/10.1029/2022JE007408

Received 31 MAY 2022
Accepted 6 SEP 2022

Author Contributions:
Conceptualization: C. M. Fedo
Formal analysis: C. M. Fedo
Investigation: C. M. Fedo
Methodology: C. M. Fedo
Validation: C. M. Fedo
Visualization: C. M. Fedo
Writing – original draft: C. M. Fedo
Writing – review & editing: C. M. Fedo

Geology and Stratigraphic Correlation of the Murray and Carolyn Shoemaker Formations Across the Glen Torridon Region, Gale Crater, Mars

C. M. Fedo[1], A. B. Bryk[2], L. A. Edgar[3], K. A. Bennett[3], V. K. Fox[4], W. E. Dietrich[2], S. G. Banham[5], S. Gupta[5], K. M. Stack[6], R. M. E. Williams[7], J. P. Grotzinger[8], N. T. Stein[8], D. M. Rubin[9], G. Caravaca[10], R. E. Arvidson[11], M. N. Hughes[11], A. A. Fraeman[6], A. R. Vasavada[6], J. Schieber[12], and B. Sutter[13]

[1]Deparment of Earth and Planetary Sciences, University of Tennessee, Knoxville, TN, USA, [2]Earth and Planetary Science, University of California, Berkeley, CA, USA, [3]U.S.Geological Survey, Astrogeology Science Center, Flagstaff, AZ, USA, [4]Department of Earth and Environmental Science, University of Minnesota, Minneapolis, MN, USA, [5]Department of Earth Science and Engineering, Imperial College London, London, UK, [6]Jet Propulsion Laboratory, California Institute of Technology, Pasadena, CA, USA, [7]Planetary Science Institute, Tucson, AZ, USA, [8]Division of Geological and Planetary Sciences, Caltech, Pasadena, CA, USA, [9]Department of Earth and Planetary Sciences, University of California, Santa Cruz, CA, USA, [10]UMR 5277 CNRS, UPS, CNES Institut de Recherche en Astrophysique at Planétologie, Université Paul Sabatier Toulouse III, Toulouse, France, [11]Department Earth and Planetary Sciences, Washington University in St. Louis, St. Louis, MO, USA, [12]Department Earth and Atmospheric Sciences, Indiana University, Bloomington, IN, USA, [13]Jacobs Technology, NASA Johnson Space Center, Houston, TX, USA

Abstract The Glen Torridon (GT) region within Gale crater, Mars, occurs in contact with the southern side of Vera Rubin ridge (VRR), a well-defined geomorphic feature that is comparatively resistant to erosion. Prior to detailed ground-based investigation of GT, its geologic relationship with VRR was unknown. Distinct lithologic subunits within the Jura member (Murray formation), which forms the upper part of VRR, made it possible to be also identified within GT. This indicates that the strata pass across the geomorphic divide between regions. Furthermore, the cross-bedded lower part of the overlying Knockfarril Hill member (Carolyn Shoemaker formation) also occurs within both VRR and GT. Correlation of both units demonstrates that the strata form a continuous stratigraphic succession regardless of large-scale geomorphic expression. The lithologic change from mudstone (Jura member) to cross-bedded sandstone (Knockfarril Hill member) heralds a significant shift in paleoenvironment from lacustrine to fluvial. The upper part of the Knockfarril Hill member consists of interbedded mudstone and sandstone that transitions to the overlying finely laminated mudstone of the Glasgow member, and a return to lacustrine deposition. In GT, the Stimson formation unconformably overlies the Glasgow member, where it demarks the southern boundary of GT. Contacts for each stratigraphic unit were defined and transferred to a high-resolution image base to make a geologic map and cross sections perpendicular to the NE strike. Stratal dips cannot exceed 2° NW to retain the positions of stratigraphic units in the locations they are exposed throughout GT.

Plain Language Summary The Mars Science Laboratory Curiosity rover explored a region called Glen Torridon (GT) that is located on the northwest side of a large sedimentary central mound (Mount Sharp) within Gale crater. This study analyzed the rocks within GT to (a) identify the sedimentary features, (b) determine if or how the sedimentary layers correlate between the Vera Rubin ridge (VRR) and GT regions, (c) interpret ancient environments, (d) generate a geologic map, and (e) discuss the relationship between topography and the exposure of sedimentary layers. Even though the VRR and GT regions are very different in present-day geomorphology, sedimentary layers correlate across the two regions indicating that the layers belong to a continuous sedimentary succession. Cross-bedded sandstones of the Knockfarril Hill member represent a change to fluvial from the underlying lake and lake-margin deposits of the Jura member, which represents a major shift in depositional environment. Packages of layers have distinct characteristics, which allows their distribution to be represented on a map. A geologic cross section limits the tilt of the layers to less than two degrees. We find that caution must be taken when attempting to derive primary stratigraphy only using datasets acquired from orbital platforms.

Journal of Geophysical Research: Planets

10.1029/2022JE007408

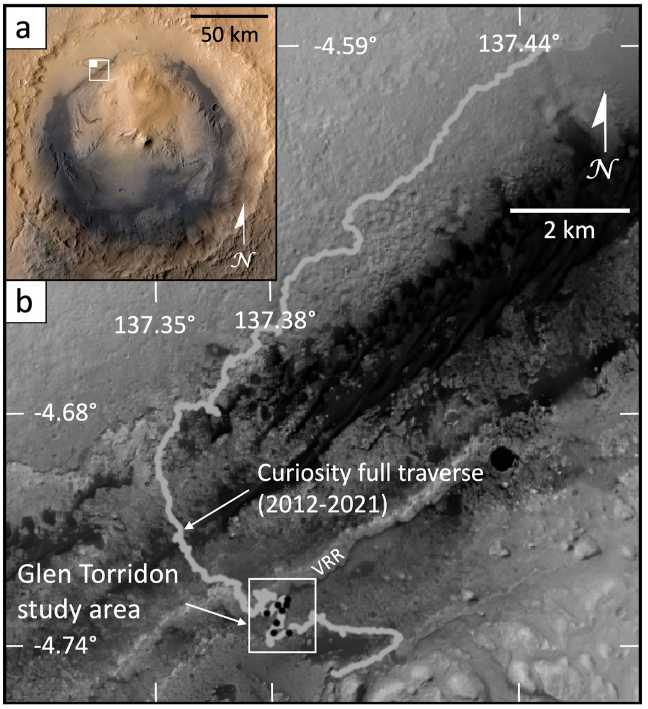

Figure 1. Location maps showing Gale crater, Mars and the traverse of Curiosity. (a) Gale crater, with inset box showing the area where Curiosity has explored. Image courtesy NASA/JPL-Caltech/ESA/DLR/FU Berlin/MSSS. (b) High Resolution Imaging Science Experiment image showing the full Curiosity rover traverse since landing. Box shows the Glen Torridon study area. VRR = Vera Rubin ridge. Image decolorized and cropped from MMGIS (Calef et al., 2017; https://mars.nasa.gov/maps/?mission=MSL).

1. Introduction

Since landing in Gale crater, which sits astride the dichotomy boundary (Figure 1), the Mars Science Laboratory (MSL) Curiosity rover has been studying the exposed sedimentary strata with the goal of determining surface paleoenvironments and their potential for habitability (Grotzinger et al., 2012). Utilizing a diverse payload of instruments capable of imaging at different resolutions and determining mineralogy and geochemical composition, the Curiosity rover has successfully provided data needed to define the stratigraphy (Figure 2) and identify fluvial (Williams et al., 2013), deltaic (Grotzinger et al., 2015), lacustrine (Edgar et al., 2020; Kah et al., 2018; Schieber et al., 2017; Stack et al., 2019), and aeolian (Banham et al., 2018, 2021, 2022) paleoenvironments within the strata comprising the north flank of Aeolis Mons (informally known as Mount Sharp). Around sol 1450, Curiosity began to follow a more southerly drive direction, ascending across bedding strike (Figure 1b), to reach the summit of Vera Rubin ridge (VRR, Fraeman et al., 2020). Images of the valley and upward slope south of VRR raised questions about how the strata of this area, designated as Glen Torridon (GT), would relate to those comprising VRR. The long-recognized presence of phyllosilicates, which are strongly connected with water both by being hydrated minerals and forming via hydrolysis, has made the GT region a prime target for exploration by Curiosity since before landing and been a motivating factor for its exploration (Bennett et al., 2022)

Stratigraphic relations play a critical role in determining the geologic and basin-fill history of a sedimentary succession. A fundamental aspect for understanding the sedimentary rocks exposed in Gale crater has been the compilation of a stratigraphic column, and its subdivision into informal members, formations, and groups on the basis of the vertical distribution of lithologies along the traverse (Figure 2). Although Curiosity has navigated laterally many kilometers, the strata are shown as a single column that incorporates any changes where they exist. Figure 2b shows the detailed lithologic column for the strata comprising GT. Given the geomorphic break that separates VRR from GT, in addition to changes in mineralogy between areas (e.g., Fraeman et al., 2013, 2016), determining how the strata of GT relate to those comprising VRR was considered critical. Namely, are the VRR and GT strata, as well as those encountered further upslope, part of a continuous stratigraphic succession or do they represent unrelated stratigraphic packages that warrant the definition of new formations?

In recognizing this need, this paper has several goals linked to documenting and interpreting the sedimentology and stratigraphy of rocks in GT, including: (a) identification of distinct lithostratigraphic units, (b) determination of stratigraphic correlations in order to show the relationship between the VRR and GT regions, (c) documentation of sedimentary features and preliminary assessment of paleoenvironments, (d) generation of a lithostratigraphy-based geologic map and cross sections to shed light on unit distribution and orientation within GT and adjacent areas, and (e) discuss the importance of integrated ground- and orbital-based observations for accurate mapping and deciphering geologic history on Mars.

2. Context and Terminology

A synthesis of the legacy geomorphic, spectral, and stratigraphic terminology is essential to contextualize prior work in this region before the stratigraphy and geology can be discussed. Figure 3 shows the (a) location of the GT region and its spatial relation to the bounding VRR and Greenheugh pediment, (b) names and locations of critical targets, (c) names of geographic features used in this paper, and (d) locations of measured stratigraphic sections. Prior to Curiosity's in situ exploration, data from orbital platforms were used to identify major features and their compositional attributes including VRR (formerly light-toned ridge or hematite ridge), and the clay-bearing unit (CBU)/phyllosilicate unit (Anderson & Bell, 2010; Fraeman et al., 2016; Milliken et al., 2010).

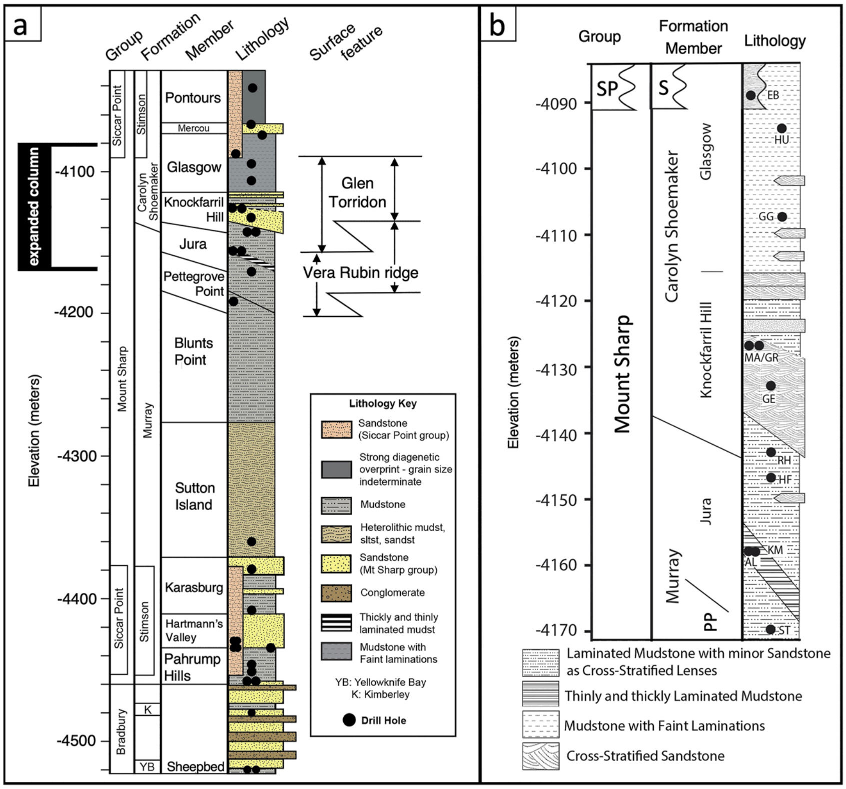

Figure 2. Stratigraphic columns for rocks of Gale crater explored by Curiosity. (a) Generalized column showing the fill section from landing to the top of rocks exposed in Glen Torridon. (b) Expanded column for the area that includes Vera Rubin ridge and Glen Torridon. Inclined boundaries between units result from contact being exposed at different elevations. SP = Siccar Point group; S = Stimson formation. Black dots are drill hole locations. ST = Stoer, AL = Aberlady, KM = Kilmarie, HF = Highfield, RH = Rock Hall, GE = Glen Etive, MA = Mary Anning, GR = Groken, GG = Glasgow, HU = Hutton, EB = Edinburgh.

Data accrued through the MSL mission has forced revisions to the terminology, which has resulted in a complex set of terms to describe various aspects of ground features, even for the same or similar units. Figure 4 illustrates the relationship between the three different groups of terminology (geomorphic, spectral, stratigraphic) as they have been used in previously published papers.

Names for specific targets and stratigraphic members follow the MSL naming convention for the Torridon quad. Prior to landing, the team developed a geologic map based on orbital data and divided the landing ellipse into quadrangles. The Torridon quad is named after a small village in the Scottish Highlands. Targets that MSL investigated within this region are named after localities across Scotland, with uncommon exceptions for names used to honor prominent figures in planetary and geosciences.

One set of terminology is geomorphic based. The GT region, the target area for the present study area, forms an approximately NE/SW-oriented trough-shaped geomorphic feature bounded on the north by VRR and to the south by the Greenheugh pediment, delineated with red contacts (Figure 4a). VRR represents a NE/SW-oriented topographic ridge possessing a sloping NW face with a steep gradient on the SE side that forms the boundary with GT (northernmost red line, Figure 4a). The geomorphic ridge also carries a strong spectral signature for hematite (Fraeman et al., 2016, 2020), linking compositional and geomorphic data. The GT region is marked by a topographic valley, or trough, that forms the north margin of GT that gradually ascends to the south to elevations well above the height of VRR along a perpendicular line (Figure 4b). The southern margin of GT is bounded by an escarpment with a sandstone that caps the Greenheugh pediment, a sloping, sandstone-capped feature that forms a near-vertical, small cliff (red line, Figure 4). This capping sandstone contains meter-scale crossstratification and is interpreted to be an up-slope continuation of the Stimson formation (Banham et al., 2022). This unit, originally mapped as the “mound-skirting unit” by Anderson and Bell (2010), is noted as having high thermal inertia (Fraeman et al., 2016).

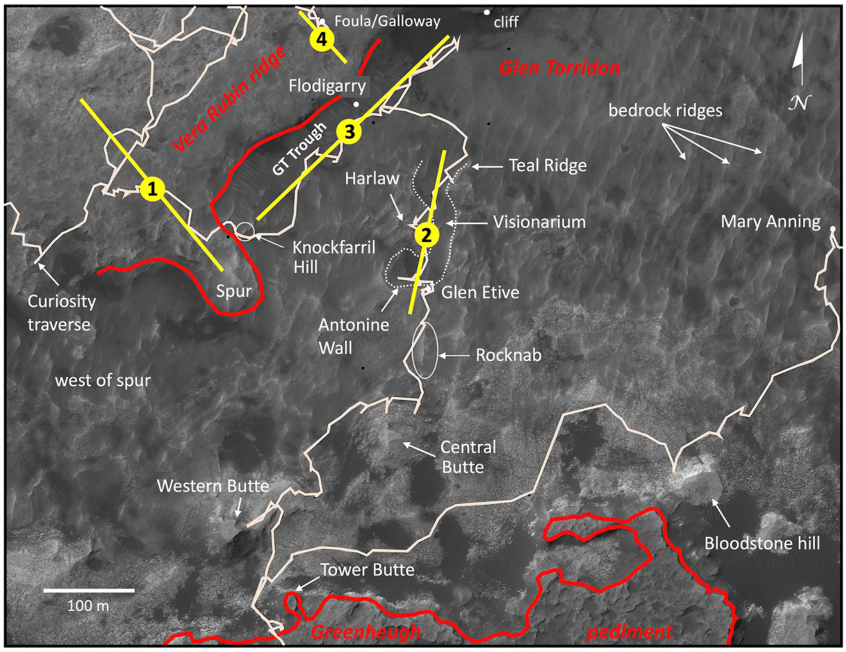

Figure 3. Map of part of the Glen Torridon (GT) study area showing common place names and specific target names in the study area. Yellow lines 1–4 show approximate locations of described measured sections. Rover traverse shown in pale orange. High Resolution Imaging Science Experiment base image. Bold red lines define the boundaries of the GT region. Dashed line traces outline of the "Visionarium." Image decolorized and cropped from web-based multi-mission GIS for MSL (Calef et al., 2017; https://mars.nasa.gov/maps/?mission=MSL).

Based on spectral characteristics, much of the region now called GT had been recognized as having an important phyllosilicate component (Anderson & Bell, 2010; Fox et al., 2018; Fraeman et al., 2016; Milliken et al., 2010). In the exploration of GT, the CheMin and SAM-EGA instruments confirmed the presence of significant proportion (6–34 wt. %) of dioctahedral phyllosilicates (Thorpe et al., 2022).

Just prior to Curiosity's arrival in GT, the team recognized three subdivisions within GT based on broad geomorphic similarities and spectral characteristics. The northeastern extent of GT associated with the CBU was divided into a smooth-ridged unit with distinct NNE/SSW-trending ridges (Stack et al., 2022), and a fractured unit with more topographic relief but less prominent ridges (light blue lines in Figure 4). From both orbital and ground perspectives, the "fractured intermediate unit" (FIU) that forms the southernmost part of GT is geomorphologically distinct with locally high topographic relief (contains prominent buttes) and has a comparatively higher albedo relative to the other GT units. The FIU, which abuts against the Greenheugh pediment, does not exhibit clear signatures of clay minerals in data sets taken from orbital platforms (He et al., 2022) clearly separating it from the fractured CBU.

The legacy names described above are commonly used in previous work, but now are being superseded by terms that incorporate new geomorphic (Hughes, 2021) and stratigraphic units (discussed in detail below) derived in part from detailed ground-based work connected to larger-area imagery. For example, Hughes (2021, 2022) has generated a highly refined geomorphic map of the GT region that recognizes 15 different units, whose features point to landscape development driven by wind erosion. Based on Hughes (2021, 2022), Christian et al. (2022) have used 12 m/pixel Compact Reconnaissance Imaging Spectrometer for Mars (CRISM) data to build maps that demonstrate correlation between surface geomorphology and apparent thermal inertia.

The other set of terminology is based on lithostratigraphy. Exploration of the geology and stratigraphy at ground level provided the detailed observations necessary to define stratigraphic units based on lithology, a practice done since the beginning of the mission (e.g., Grotzinger et al., 2015), that, for reasons described below, is intended to replace the legacy geomorphic and spectral terminologies. The generalized cross section (Figure 4b) shows the succession of stratigraphic units comprising both VRR and GT. The details of this succession form the main purpose of this paper and are discussed below. Some units previously identified via geomorphology (e.g., VRR,

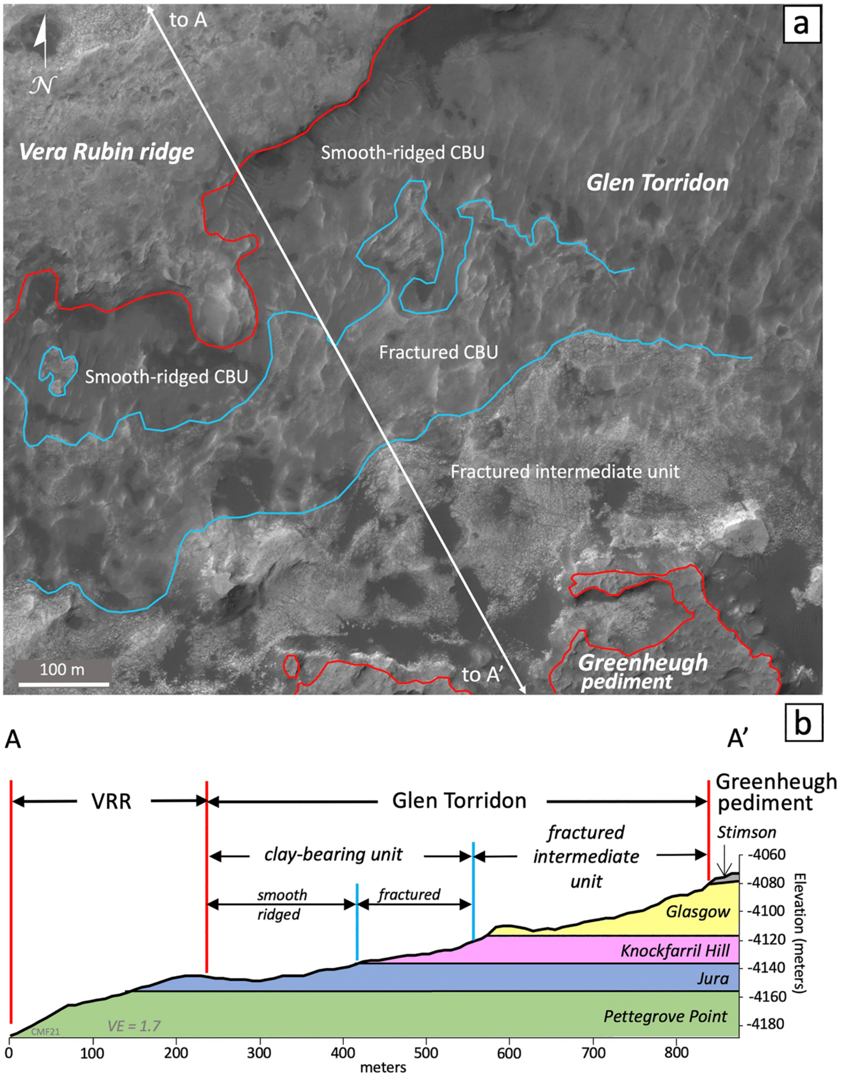

Figure 4. Map and simplified cross section of part of the study area showing legacy terminology in Glen Torridon (GT). (a) Map showing the main subdivisions of GT based on geomorphology. Line shows position of cross section in (b). CBU = clay-bearing unit. (b) Simplified cross section showing stratigraphic units (Pettegrove Point through Stimson formations) and boundaries where previous commonly used terms intersect stratigraphy. VE = vertical exaggeration. VRR = Vera Rubin ridge. Note that the VRR—GT and CBU—fractured intermediate unit boundaries do not coincide with stratigraphic units. Image decolorized and cropped from multi-mission GIS for MSL (Calef et al., 2017).

FIU) or spectral characteristics do not necessarily coincide with stratigraphic (formation, member) boundaries. For example, the southern boundary of VRR (upper red line, Figure 4a), though topographically prominent, possesses no stratigraphic significance because strata of the Jura member (Murray formation) continue across the geomorphic contact into GT (discussed in Sections 4 and 5). Likewise, the boundary between the fractured clay-bearing (CBU) unit and the FIU within GT (blue line, Figure 4) occurs within the Knockfarril Hill member of the Carolyn Shoemaker formation. Owing to the importance of stratigraphic designations (Figure 2) based on direct, ground-level observation, legacy terminology is only used in this paper to identify specific topographic features, geographic regions, or areas with consistent surface textures.

3. Methods

The data used in this paper originate from instrumentation aboard the Curiosity rover, the details of which can be found in Grotzinger et al. (2012). Individual images and image mosaics are used in this paper to document critical stratigraphic relationships, sedimentary structures, and lithologies (sandstone vs. mudstone). The images come from the Navigation cameras (Navcams; Maki et al., 2012; Maki, 2018) and Mast cameras (Mastcams—M34 left, M100 right; Malin, 2013; Malin et al., 2017), which are found at the top of the rover's remote sensing mast and the Mars Hand Lens Imager camera (MAHLI; Edgett et al., 2012; Edgett, 2013) located on the instrument turret at the end of the robotic arm at the front of Curiosity. During the campaign and ahead of actual exploration, several prominent locations were remotely observed using the Remote Micro-Imager (RMI) subsystem of the ChemCam instrument (Wiens et al., 2012, also located atop the remote-sensing mast) as a telescope to perform observations from a distance (Le Mouélic et al., 2015). The RMI was also used as a complement to MAHLI images to assess fine-scale detail such as texture and grain size. Images that cover larger areas of the GT region come from the High Resolution Imaging Science Experiment (HiRISE; Calef & Parker, 2016; Calef et al., 2019; McEwen, 2005; McEwen et al., 2007) aboard Mars Reconnaissance Orbiter (MRO).

The stratigraphic column (Figure 2), which is divided into informal lithostratigraphic units, represents the product of continual revision from early in the mission (e.g., Grotzinger et al., 2015) as Curiosity has ascended to higher elevations. As with columns compiled from sedimentary successions on Earth (e.g., Boggs, 2012), it summarizes the lithologies and salient sedimentary features observed along the traverse. The column is informed from analysis of individual images and image mosaics acquired by the science cameras noted above. Lithostratigraphic units were defined on physical characteristics visible in outcrop, such as color, grain size, and sedimentary features (e.g., cross stratification, ripple marks, and lamination), with further documentation of post-depositional diagenetic features (e.g., concretions, cementations, veins, fractures). Using lithologies and lithologic assemblages, the column was then divided into mappable stratigraphic units representative of members, formations, and groups, although used in an informal sense.

The thickness of stratigraphic units, and thus the combined thickness for the entire column relies on the premise that the strata are approximately horizontal. Regional studies of possible stratal orientation have suggested northwest-oriented dips (away from the Gale crater central mound) that range from 2.5° to 4.5° (e.g., Kite et al., 2013; Kite et al., 2016). However, ground-based bedding orientations using Mastcam images led Stein et al. (2020) to conclude that local bedding dips occur in all directions at very shallow angles and the strata are near horizontal, so that change in elevation may be used as a proxy for stratal thickness.

A geologic map of GT was made based on ground-based observations from the rover, as defined by units represented in the stratigraphic column (Figure 2). Stratigraphic unit contacts identified from image analysis in the vicinity of Curiosity were located on a HiRISE base map. Working from a position of high confidence around Curiosity where abundant data exists, ground features, such as topographic inflections, rock colors, and fracture patterns were identified that could be observed in longer distance Mastcam and RMI images and on the HiRISE base map upon which contacts were extended. Using web-based, multi-mission GIS software for the MSL mission (MSL MMGIS; Calef et al., 2017, 2019), a topographic profile was drawn across the contact at the location of the rover traverse to correlate any local relief with unit contacts, which was common. Combining all these approaches, contacts were mapped across GT, except in one instance (eastward and westward extensions Knockfarril Hill—Glasgow member contact) where the contact could not be accurately located across the map area with imagery or specific topographic inflections most likely because of substantial diagenetic overprint (Dehouck et al., 2022).

In this case, the contact was directly observed at three locations in the region of Central and Western buttes, and then crossed at a fourth location north Bloodstone hill (Figures 3 and 10) between sols 2813 and 2816. While the contact was not directly studied at the fourth location, an estimated location is bracketed by observations between those sols where rocks could be assigned to the Knockfarril Hill and Glasgow members. Using the four anchor locations, which are separated by more than 400 m, the contact (dotted line) was drawn as a calculated plane with an orientation of 221°/2.25° NW.

4. Lithostratigraphy

Stratigraphic units that occur in the GT region belong to the Murray and Carolyn Shoemaker formations of the Mount Sharp group (Figure 2). Whereas the Murray formation comprises seven members, only the topmost (Jura member) crops out in GT. Two members of the Carolyn Shoemaker formation, the Knockfarril Hill member and the Glasgow member occur within GT. The southern boundary of GT is demarked by the base Siccar Point group unconformity (Greenheugh pediment) that separates the Glasgow member of the Carolyn Shoemaker formation from the Stimson formation, Siccar Point group (Figure 2; Banham et al., 2022).

4.1. Murray Formation

4.1.1. Jura Member

Rocks belonging to the Jura member (Figure 5) cross the geomorphic boundary between VRR and GT, as well as the significant iron-versus clay-enriched spectral boundary that coincides with VRR and GT regions (Figure 5a; Anderson & Bell, 2010; Fraeman et al., 2016; Bennett et al., 2022). Details about the sedimentology and paleoenvironments of the Jura member (and underlying Blunts Point and Pettegrove Point members) were described by Edgar et al. (2020). Generally, the Jura member consists of two mudstone facies (Facies 3 and Facies 4 of Edgar et al. (2020)), locally separated by a folded mudstone facies suggestive of syndepositional slumping (Facies 6, of Edgar et al. (2020)). These facies were defined on the northwest slope of VRR where exposure is nearly continuous. Facies 4, termed "Flodigarry facies," after a target of the same name (see location on Figure 3, also Figure 5e), forms the base of the Jura member. This unit is particularly distinctive, consisting of centimeter-scale recessive-resistant alternations of laminated maroon-and-orange mudstones/siltstones exemplified by Mastcam targets Galloway (Figure 5b) and Foula (Figure 5c, see location on Figure 3).

Outcrops of the Jura member in the GT trough are dominated by a smooth bedrock that typically weathers into cm-scale pieces of rubble (Caravaca et al., 2022; Dehouck et al., 2022). Scattered broken slabs expose up to several decimeters of local relief with less common meter-scale ridges (Figure 5a) making detailed descriptions of the lithologies difficult. Most of the exposures are dominated by laminated mudstone-siltstone, with some locally occurring millimeter-to centimeter-scale ripple cross laminations (Caravaca et al., 2022) and lenses of decimeter-thick resistant ridges that display plausible cross stratification (Figure 2b, arrow on Figure 5a) that represent a transition to the overlying cross-stratified sandstone of the Knockfarril Hill member (Carolyn Shoemaker formation; Caravaca et al., 2022; see below). Within the GT trough, mudstone units, in particular, are exposed as numerous, small, north-northeast trending bedrocks ridges, likely the result of directed wind erosion and not exposed primary depositional bedforms (Stack et al., 2022). Bedrock targets Flodigarry (Figures 3 and 5e), for which the facies is named, and Woodland Bay (Figure 5d) display characteristic centimeter-scale interbeds of maroon and orange mudstones/siltstones, which are characteristic for this facies (Caravaca et al., 2022; Edgar et al., 2020). Imaging of the south face of VRR (cliff location on Figures 3 and 5f) shows the two dominant members of the Jura member Flodigarry facies (Facies 4) and overlying Facies 3 directly project through VRR. An expanded view of the lower part of the cliff (Figure 5g), reveals the distinct centimeter-scale alternations identified in close-up images.

4.2. Carolyn Shoemaker Formation

4.2.1. Knockfarril Hill Member

The base of the Carolyn Shoemaker formation is identified by a significant lithologic change from recessive rubble-covered mudstone of the underlying Jura member (Murray formation) to ridge-forming sandstone followed by interstratified mudstone and sandstone of the Knockfarril Hill member (Carolyn Shoemaker formation; Figures 2 and 6). The member, divided into two lithofacies, is approximately 25 m thick.

The lower lithofacies is approximately 10 m thick and is characterized by decimeter-to locally meter-scale trough (Figures 6b and 6c) and tabular (Figure 6d) cross-stratified sandstone. Based on outcrop appearances, this lithofacies has minimal interbedded mudstone. The best outcrop of this facies occurs as a nearly 40 m wide, 1–2 m tall, continuous, lateral exposure at the Antonine Wall location (Figure 3). Bedding in this location is less than about 10 cm thick and consists of stacked toesets of tabular-tangential cross-stratification. The top of this unit was drilled (Glen Etive) and studied extensively for (Dehouck et al., 2022; O'Connell-Cooper et al., 2022) and potential preserved organics (McAdam et al., 2022). While grain-size is difficult to determine through this interval, high-resolution MAHLI mosaics taken from centimeters from the outcrop surface, along with ChemCam RMI image mosaics, locally show dimpled outcrop textures suggestive of fine-to-medium sand.

A second lithofacies consisting of approximately 10 m of interbedded sandstone and mudstone overlies the lower cross-stratified facies (Figure 2). Sandstones occur as decimeter-to-meter thick bodies that can be traced laterally

10.1029/2022JE007408

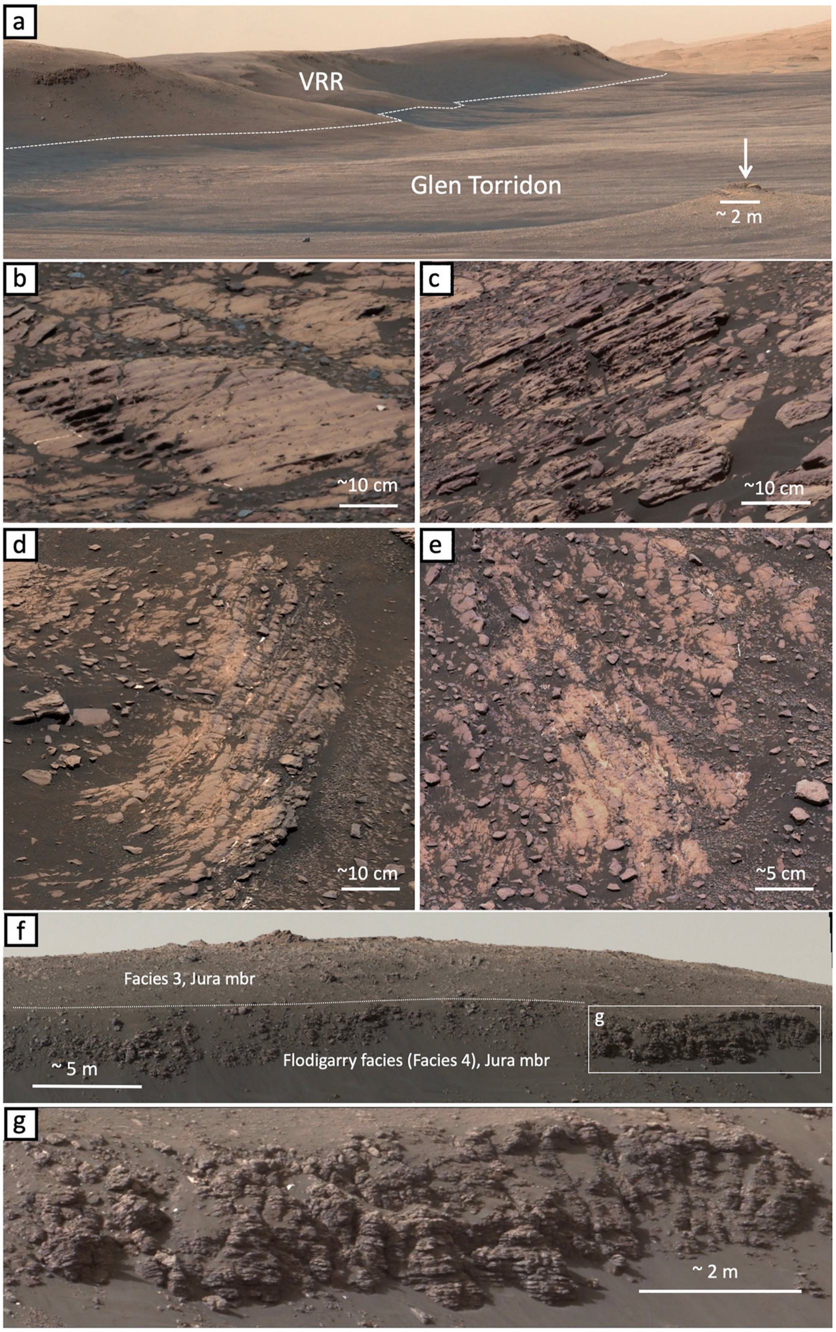

Figure 5. Cropped images showing key features of the Jura member (Murray formation). (a) Mastcam M34 mosaic of view to the east showing the geomorphic boundary between Vera Rubin ridge (VRR) and Glen Torridon (GT), and the prominent trough in GT. White arrow identifies a likely sandstone body. Sol 2354. Image information: sequence mcam12490.0000a, drive direction 5 × 1 L0. (b) Mastcam 34 image of Flodigarry facies on Vera Rubin ridge, Galloway target. Sol 2013. Image information: sequence mcam10610.0000a, galloway 4 × 1 Lall. (c) Mastcam 100 image of Flodigarry facies on Vera Rubin ridge, Foula target. Sol 2013. Image information: sequence mcam10615.0000a, foula 3 × 1 R0. (d) Mastcam 34 image of Flodigarry facies in GT, Woodland Bay target. Sol 2359. Image information: sequence mcam12506.0000a, woodland bay 9 × 1 L0. (e) Mastcam 100 image of Flodigarry facies in GT, Flodigarry target. Sol 2357. Image information: sequence mcam12498.0000a, flodigarry stereo 23 × 2 L0 R0. (f) Mastcam M100 mosaic of Jura member exposed on the south side of VRR showing Flodigarry facies and facies 3. Sol 2389. Image information: sequence mcam12685.0000a, ripple field stereo 30 × 4 L0 R0. (g) Expanded image of part of (f) showing alternations characteristic of Flodigarry facies. Additional color stretching by authors. All images courtesy Malin Space Science Systems.

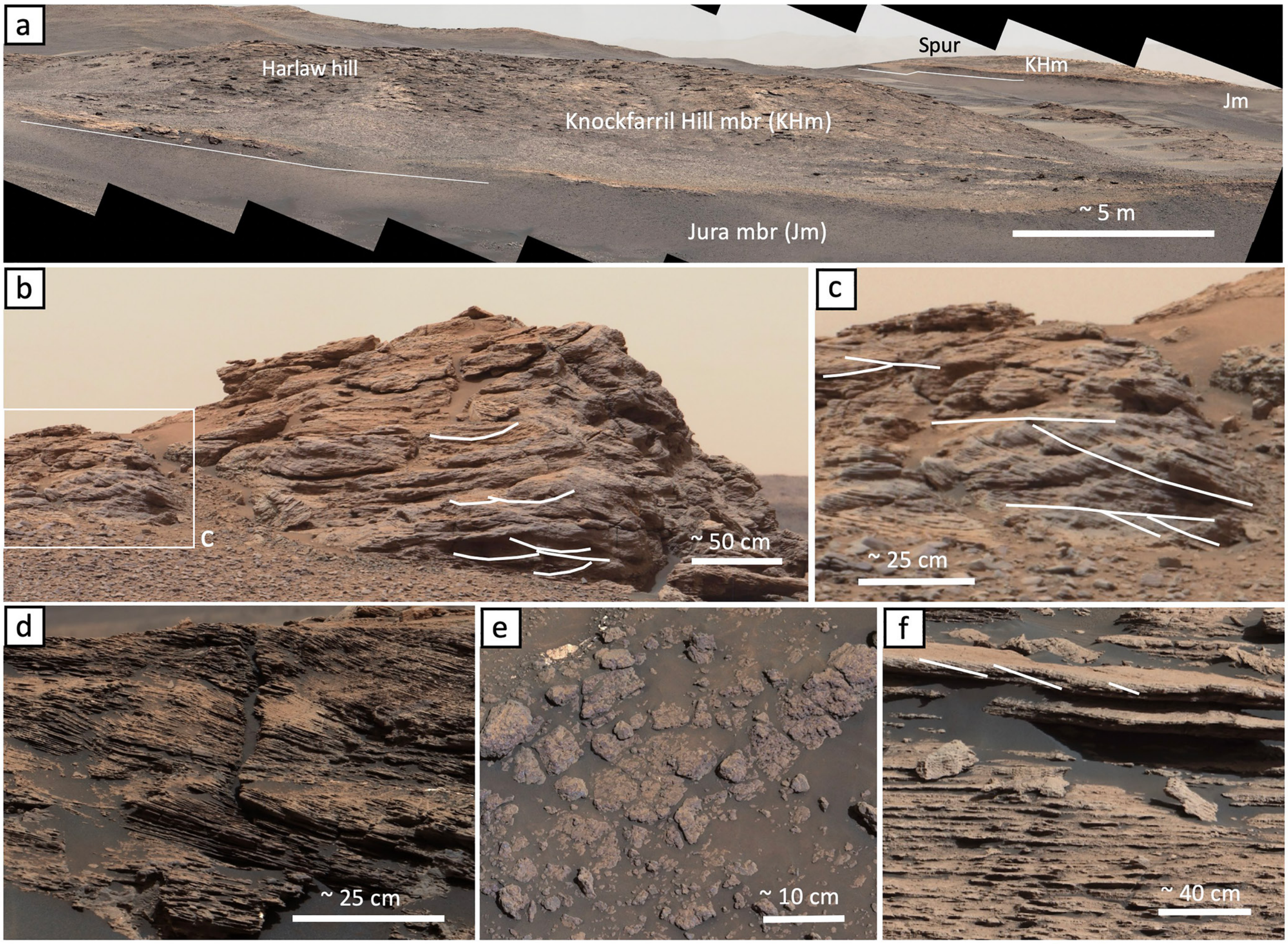

Figure 6. Cropped images showing key features of the Knockfarril Hill member (Carolyn Shoemaker formation). (a) Mastcam 100 image looking west from Teal Ridge showing the contact between Jura (Jm) and Knockfarril Hill (KHm) members at Harlaw hill (foreground) and the same contact in the distance at the Spur location. Sol 2443. Image information: mcam12952.0000a, visionarium stereo 10 × 2 L0 R0. (b) Mastcam 100 image of the Knockfarril Hill showing cross stratification. Sol 2311. Image information: sequence mcam12341.0000a, knockfarril_hill_stereo_2 × 1_L0_R0. (c) Expanded view of part of (b) with white lines tracing cross-stratification and erosional truncation surfaces between sets. (d) Mastcam M100 image showing cross stratification exposed at the base of KHm at Teal ridge. Sol 2447. Image information: sequence mcam12976.0000a, south walls stereo 5 × 2 L0 R0. (e) Mastcam M34 image showing interbeds of maroon laminated mudstone showing vuggy texture in the upper part of the member. Sol 2563. Image information: sequence mcam13455.0000a, workspace 3 × 2 L0. (f) Mastcam 100 image showing laminated mudstone overlain by tabular-planar cross-stratified sandstone on Central butte below contact with Glasgow member. Sol 2572. Image information: sequence mcam13507.0000a, hunda stereo 9 × 2 L0 R0. Additional color stretching by authors. All images courtesy Malin Space Science Systems.

for tens-to-hundreds of meters based on sedimentary structures and/or outcrop expression. One sandstone bed (target Rocknab, location on Figure 3) at −4,125 m elevation forms the core of an erosional bedrock ridge that is likely in-family with those expressed in the Jura member at lower elevations in GT (Stack et al., 2022). The best exposure of sandstone beds occurs at the base of Central butte (location on Figure 3), where a 2 m thick interval displays beds of centimeter-scale amplitude and near meter-scale wavelength symmetrical ripple marks, and several centimeter-thick beds of tabular-planar cross stratification (white lines, Figure 6f). Interbedded mudstones are poorly exposed, limited to small broken-up outcrops composed of trains of dark purple fragments parallel to bedding (Figure 6e). Individual fragments show a vuggy texture and millimeter-thick laminations, similar to those in the Jura, Pettegrove Point, and Blunts Point members (Edgar et al., 2020).

4.2.2. Glasgow Member

The Glasgow member (Figure 7) overlies the Knockfarril Hill member with a sharp contact where Curiosity captured close-range high-resolution images near the base of Central butte (Figure 3). Although a distinct change in outcrop and geomorphic expression occurs at the base of Central butte that denotes the boundary of the "FIU"

10.1029/2022JE007408

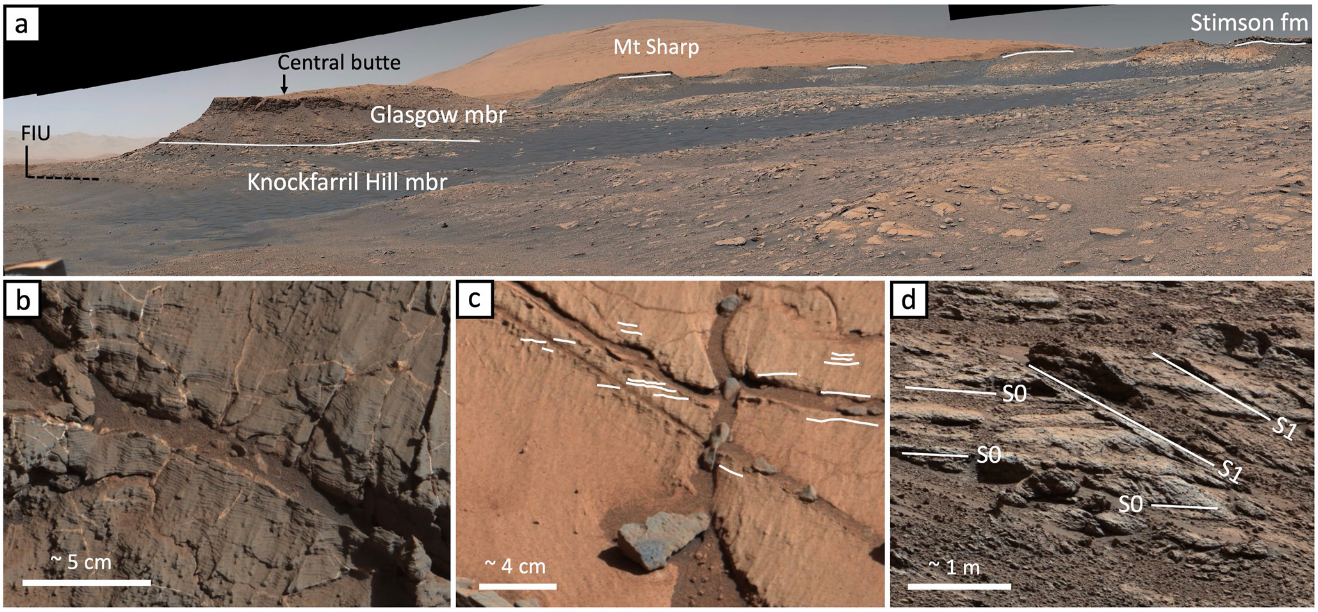

Figure 7. Images showing key features of the Glasgow member (Carolyn Shoemaker formation). (a) Mastcam 100 mosaic looking east showing the contact between the Knockfarril Hill—Glasgow members and Glasgow—Stimson formation (Siccar Point group). Note contact position of the "fractured intermediate unit." Mount Sharp in the distance. Sol 2600. Image information: sequence mcam13655.0000a, glen torridon stereo 360 p2 L0 R0. Central butte is ∼10 m in local relief for scale. (b) Mastcam 100 mosaic showing laminated mudstones characteristic of the Glasgow member. Sol 2613. Image information: sequence mcam13735.0000a, ghrudaidh workspace 4 × 3 L0 R0. (c). Mastcam 100 mosaic showing laminated mudstones characteristic of the Glasgow member. Sol 2642. Image information: sequence mcam13832.0000a, abernethy ccam stereo 4 × 3 L0 R0. (d) Primary bedding (S0) and fracture (S1) relationship in Glasgow member, Western butte. Sol 2611. Image information: sequence mcam13724.0000a, western butte stereo 11 × 2 L0 R0. Additional color stretching by authors. All images courtesy Malin Space Science Systems.

(black dashed line, Figure 7a), the basal contact of the Glasgow member occurs higher in the stratigraphy and so does not coincide with legacy map units (Figures 3 and 4). The thickness of this member varies because the Stimson formation rests on an unconformity that dips at an angle of approximately five degrees at this location (Bryk et al., 2019). The best exposures of the Glasgow member occur on the steep flanks of several buttes (e.g., Central butte, Western butte, Figures 3 and 7a) and the steep slope beneath the Stimson formation unconformity (Figure 7a).

Rocks of the Glasgow member are dominated by gray rocks, inferred to be mudstones, that display millimeter-scale laminations (Figures 7b and 7c). Where dust cover is particularly abundant, laminations are only faintly visible, and generally are best exposed along fractures or sharp edges of outcrops (Figure 7c). Glasgow member strata also contain clusters of northward-dipping penetrative fracture sets (S1, Figure 7d) that are locally prominent enough to obscure primary depositional layering (S0, Figure 7d).

4.3. Stratigraphic Correlation

Curiosity descended into GT via the Knockfarril Hill outcrop (Figure 3), passing across the distinct geomorphic and spectral boundaries that separate VRR and GT. Notwithstanding the long-recognized and profound differences between these two regions, it was not known what rock units would be exposed in GT, and whether they would allow delineation of stratigraphic relationships to VRR. As described above, in the GT trough, rocks very similar in appearance to the Galloway and Foula targets occur as centimeter-high outcrops broken into plates. Mastcam targets Woodland Bay (Figure 5d) and Flodigarry (Figure 5e) directly resemble Galloway and Foula, and furthermore, occur at similar elevations on VRR and in GT consistent with them being the same units. Additionally, the cliff exposure on the south side of VRR (Figures 5f and 5g) provides the connection that establishes a clear stratigraphic correlation between VRR and GT for the Jura member.

Figure 8 illustrates the correlation of the Jura member across four measured sections that span across VRR and GT. Column 1 (SW VRR) shows the section that intersects the Spur, the highest elevation area part of VRR,

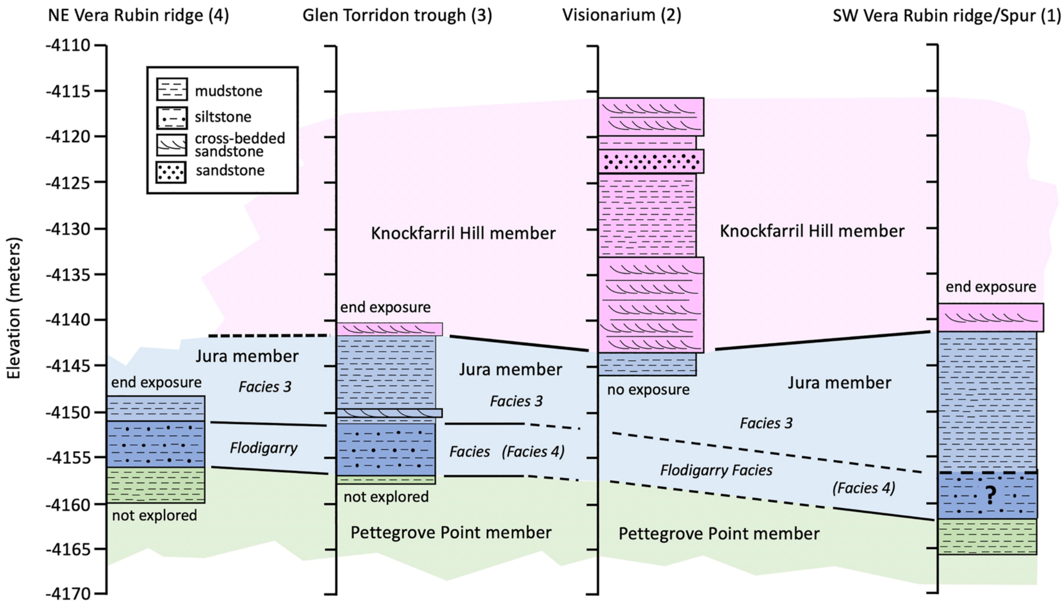

Figure 8. Detailed measured columns and stratigraphic correlations that link Vera Rubin ridge and Glen Torridon. Numbered section locations noted on Figure 3.

beginning with the Pettegrove Point member (Murray formation) at the base and topping out with rocks of the Knockfarril Hill members (Carolyn Shoemaker formation) at the summit of the Spur. Without observation of the Pettegrove Point—Jura member contact, Flodigarry facies rocks are presumed to be present based on exposures both east and west of the section line, and overlain by laminated mudstones of Facies 3, which is also observed at column 4 (NE VRR).

In the trough at the north margin of GT (column 3), the identification of Jura member facies directly correlates with identical exposed facies on VRR. Curiosity traversed southeast and uphill from about the Flodigarry target location toward the Visionarium (Figure 3) across rocks that show no change from the base of the GT trough, and so are interpreted as belonging to the Jura member (Facies 3). Consequently, we correlate the Jura member directly across the VRR—GT boundary, suggesting that the regions are stratigraphically connected and that the Jura member is a widespread depositional unit.

At the summit of VRR, where the traverse descends into GT (Figure 3), Curiosity imaged the target Knockfarril Hill, an isolated, meter-tall outcrop with profuse cross-stratification (Figures 6b and 6c). This outcrop is erosionally detached but similar in appearance to rocks that comprise the top of the column 1 ("Spur" location on Figures 3 and 8). Curiosity next encountered cross-bedded sandstone at Harlaw rise and Teal ridge at the northern end of a prominent valley informally termed the "Visionarium" (Figure 3). These sandstones overlie dark mudstones of the Jura member (Figure 6a) and occur near the base of column 2 (Figure 8). Based on the profound change in lithology, distinct sedimentary structures, and similar elevations, we recognize this as a widespread stratigraphic interval that correlates across VRR and GT (Figure 8) and marks the beginning of a new depositional episode. Correlation of the Jura and Knockfarril Hill members provides strong evidence that, despite dramatic changes in geomorphology and surficial composition as determined from orbital platforms, the stratigraphy exposed in GT represents a continuation of the succession leading up to VRR (Figure 2a).

4.4. Paleoenvironments

Lithologies and sedimentary structures of the different members allow insights about their sedimentary environments and paleogeography. Two critical units, the Jura member (Murray formation) and the Knockfarril Hill member (Carolyn Shoemaker formation), illustrate the range of preserved paleoenvironments in GT.

Sedimentary features including pervasive laminated mudstone led Edgar et al. (2020) to envision an overall lacustrine depositional setting for the Jura member. The upper part (Facies 3) exposed in GT shows lenses of

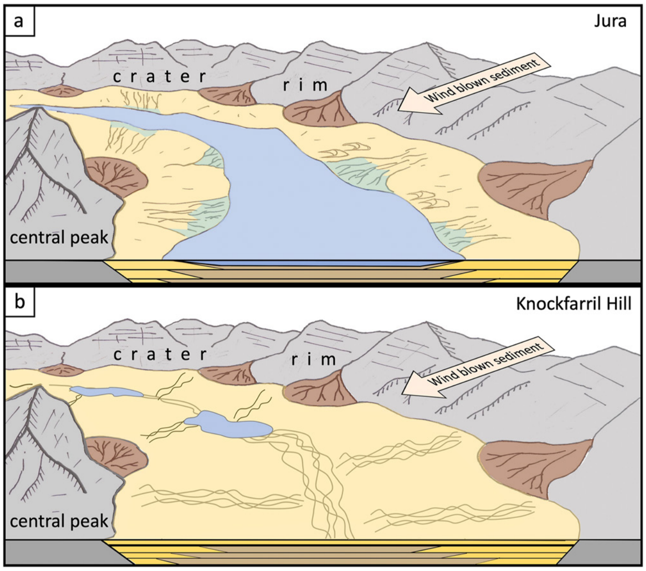

Figure 9. Cartoons show the inferred paleogeography for the Jura and Knockfarril Hill members. For scale, mountains across top of images represent the crater rim, while the mountain in the lower left represents rocks of a central uplift. Area represented by the Glen Torridon region is very small. In map view, basaltic bedrock is shaded gray. Alluvial fan deposits emanating from mountain fronts are shaded brown. Fluvial and Aeolian deposits are shaded yellow. Delta deposits are shaded pale blue-green. Lake deposits are shaded blue. Cross-sectional views show stratigraphy (fluvial and Aeolian shaded yellow, lake shaded light brown). (a) Jura member, Murray formation. (b) Knockfarril Hill member, Carolyn Shoemaker formation. Note the thicker line in the cross-section represents the contact between the Jura and Knockfarril Hill members. Glasgow member paleogeography would look similar to the Jura member.

cross-stratified sandstones (Caravaca et al., 2022), suggestive of comparatively coarse sediment delivery to the margin of, or into, a standing body of water.

By contrast, the base of the Knockfarril Hill member is about 10 m thick and is dominated by cross-stratified sandstone. Coupled with a lack of channel forms and minimal interbedded mud (in the first 10 m), the observations are consistent with stacking fluvial barforms in a braided alluvial environment similar to those seen in vegetation-free landscapes on Earth in the rock record (e.g., Long, 2011; Muhlbauer et al., 2020).

Figure 9 shows two simplified paleogeographic models for the overall configuration of depositional environments at the time of Jura member (Murray formation) and the Knockfarril Hill member (Carolyn Shoemaker formation), with lacustrine deposition being fed from the rim (and center) of Gale crater by alluvial systems. The Jura member is viewed in Figure 9a as a large lake where a principal depositional process was suspension fallout (Edgar et al., 2020) of sediment delivered through coastal deltas. Although not preserved at present erosional levels, the most likely larger scale configuration is that the lake body experienced progressive filling by alluvial deposition from the margins and potentially a significant volume of sediment carried in from outside the crater. Overlying rocks of the Knockfarril Hill member define a distinctly mappable contact (discussed below) indicating widespread sandstones likely rest sharply on the Jura member.

Given the correlation that connects the different sections (Figure 8), we interpret the widespread nature of the lower part of the Knockfarril Hill member as representing a sizable braidplain that supplanted antecedent lacustrine environments (Figure 9b), indicative of a paleoenvironmental shift comparable to that recorded between the Bradbury and Mount Sharp groups (Grotzinger et al., 2015; Stack et al., 2019) and facies shifts in lower members of the Murray formation (Gwizd et al., 2022). The cross-sectional view shows a heavy line separating mudstones from the sandstones consistent with some amount of erosion, even if it is only linked to the basic erosive nature of the fluvial environment itself. The intercalated sandstones and mudstone higher in the Knockfarril Hill member are thought to represent alternations between expanding and contracting episodes of lake deposition prior to a return to lake widespread lacustrine deposition of the Glasgow member, possibly resembling the paleogeography of the Jura member.

5. Geologic Mapping

5.1. Background

Utilizing (a) the distinct lithologies that define the stratigraphic succession (Figure 2), (b) near- and far-distance imaging, (c) significant direct observation laterally and vertically, and (d) specific, consistent trends in local topographic relief (geomorphology) connected to lithologic changes, we present a member-based geologic map (Figure 10, Fedo et al., 2022) and cross section (Figure 11) through the units comprising GT. The combined detailed exploration of VRR and GT generated an extensive data set of observations along and across strike for each stratigraphic member. Identifying contact relationships (lithology, local geomorphology, color variation etc.) proximal to the rover in multiple locations permits unit contacts to be traced with confidence laterally using the support of longer distance imagery and HiRISE images. Confidence in contact positioning far from the traverse strike lessens using imagery alone.

5.2. Pettegrove Point—Jura Members Contact

Details of the Pettegrove Point—Jura members (Murray formation) contacts were defined on the north side of VRR (Edgar et al., 2020). Having crossed and examined the contact at multiple locations along the summit ridge

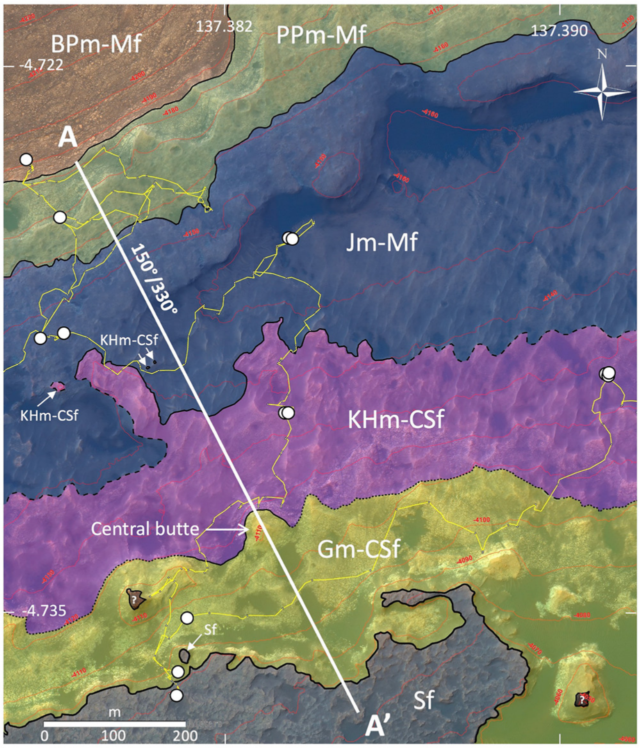

Figure 10. Geologic map of the Glen Torridon region using stratigraphic units shown in Figure 2. Note A–A' line for the cross section. Mf = Murray formation, BPm = Blunts Point member, Jm = Jura member, KHm = Knockfarril Hill member, Gm = Glasgow member, Sf = Stimson formation. Solid line, contact well located; dashed line, contact location approximated; dotted line, contact drawn as best fit calculation. White dots = locations of drill samples. Thin yellow line, Curiosity traverse path. Question marks identify units whose stratigraphic position is uncertain.

of VRR (Figure 10), the contact was readily identified, particularly because the Flodigarry facies of the Jura member (Facies 4, Edgar et al., 2020) is lithologically so distinctive relative to underlying Pettegrove Point member. There also is a consistent local topographic step due to the somewhat greater induration of the Jura member, probably due to extensive diagenetic alteration of VRR (Bristow et al., 2021; Fraeman et al., 2020; Frydenvang et al., 2020; L'Haridon et al., 2020). The contact that defines the base of the Jura member loosely follows the −4,160 m contour line, consistent with minimal dip across a strike distance of nearly 1 km. Within the northeast part of the explored GT trough, erosion related to the generation of the present topography cuts deeply enough to expose Flodigarry facies rocks (Figures 5d and 5e), but does not reach down to the Pettegrove Point member. Thus, only Jura member strata crop out in the GT trough (Figure 10).

5.3. Jura—Knockfarril Hill Members Contact

The contact between the Jura member (Murray formation) and the Knockfarril Hill member (Carolyn Shoemaker formation) was examined closely at three locations in the study area, near the top of the Spur, and at two locations in the "Visionarium" (Teal ridge and Harlaw, Figures 3, 6a, 10, and 12a). At all locations, the contact between the Jura is sharp and flat (Figures 6a and 12a), although the contact does span about 5 m of elevation across GT (Figure 8). The contact can be interpreted as erosive, which would be consistent with incision of fluvial transport over mud or poorly lithified mudstone.

In the area between the Spur and Teal ridge, the contact is well-located given the distinctly different outcrop expression of the two units; however, the contact is less clear both east and west of those locations (dashed lines). Directly east of Teal ridge the contact is similarly well located, but further to the east, uncertainty increases as images become long distance, are along strike, and obstructed by ridges. Cross-stratified sandstones similar to those at Knockfarril Hill and Teal ridge occur at the Mary Anning location (Figures 3 and 10), so this basal unit extends eastward to at least that location. Curiosity did not re-cross the contact near Mary Anning, so the contact location was inferred using outcrop pattern. The same is true for the extension of this contact west of the Spur. Across the study area, the contact loosely follows the −4,140 m elevation contour (Figure 10), except for the far eastern projection.

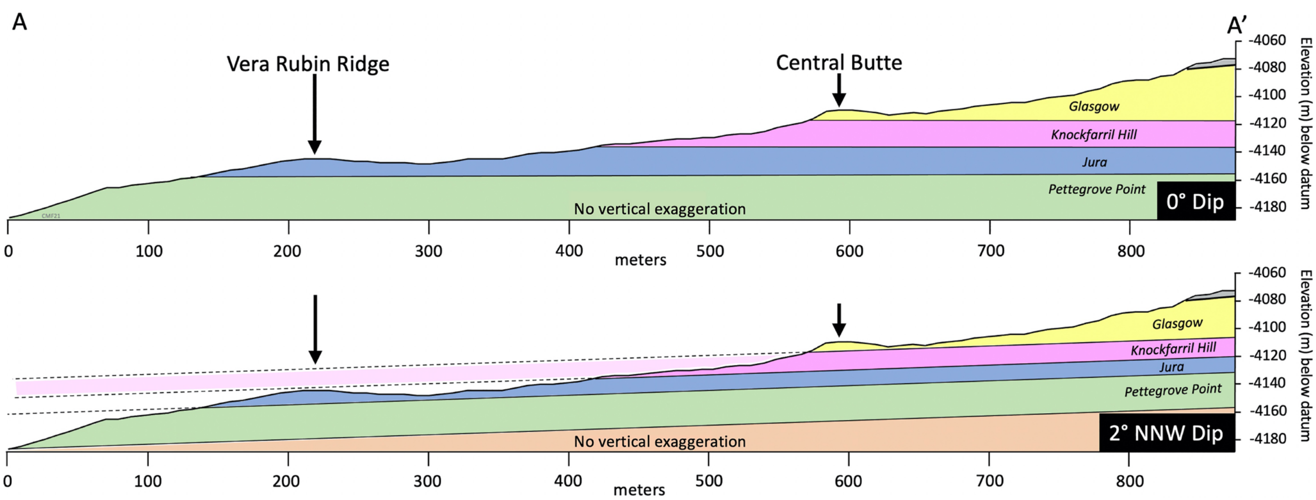

Figure 11. Geologic cross sections along the line A–A' on the geologic map. Note positions of Vera Rubin ridge and Central Butte. No vertical exaggeration. Upper cross section shows stratigraphic units with 0° dip. Bottom cross section shows stratigraphic units with 2° NNW dip (perpendicular to strike on geologic map).

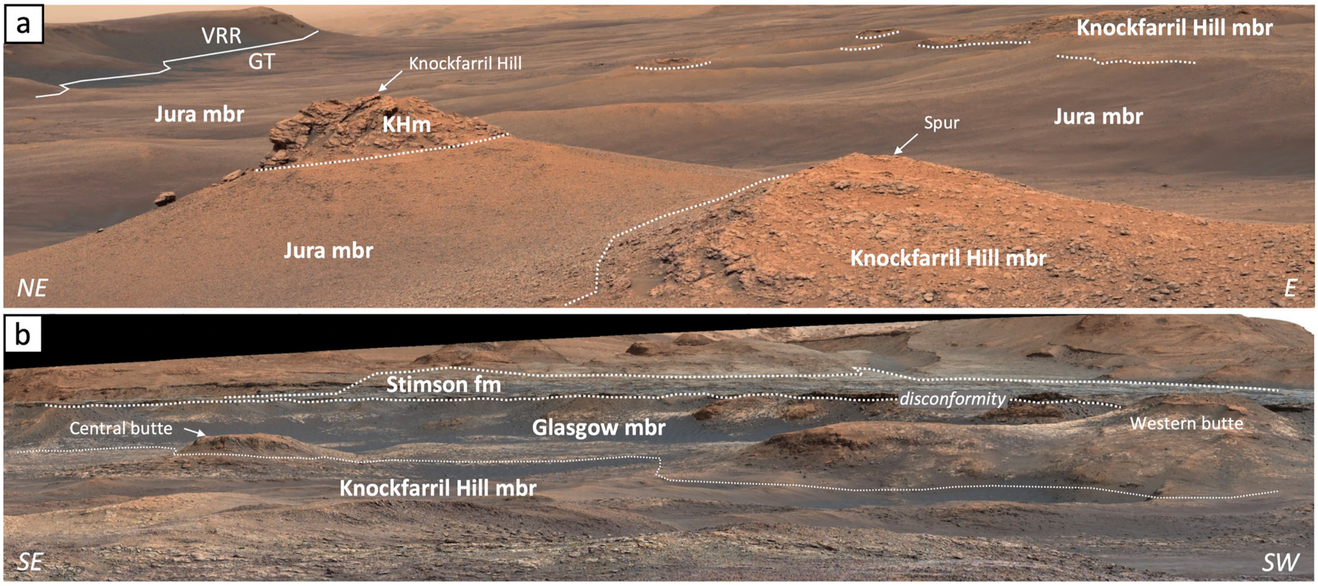

Figure 12. Mastcam 34 mosaic images showing geologic contacts (dotted lines) between mapped stratigraphic units in Glen Torridon. (a) Easterly view of the Glen Torridon trough from the top of the Spur showing contacts between Jura and Knockfarril Hill members. Note location of Knockfarril Hill and Spur outcrops. Small cliff exposure of Knockfarril Hill is approximately 1.5 m tall. Sol 2304. Image information: sequence mcam12312.0000a, drive direction 5 × 1 L0. (b) Southerly view of Glen Torridon from Vera Rubin ridge showing the contacts between the Knockfarril Hill and Glasgow members, and disconformity between the Glasgow member and Stimson formation (Greenheugh pediment). Flat summit of Central butte is ~30 m across for scale. Sol 2264. Image information: sequence mcam12110.0000a, lairig ghru stereo 10 × 2 L0 R0. Color stretching by authors. All images courtesy Malin Space Science Systems.

5.4. Knockfarril Hill—Glasgow Members Contact

The contact between the Knockfarril Hill and Glasgow members, both part of the Carolyn Shoemaker formation, is identified and best exposed on the steep lower slope of Central butte (Figures 3, 7a, 10, and 12b) and on the lower slope of Western butte (Figures 3 and 7a). There, the upper part of the Knockfarril Hill member consists of alternating, meter-thick, packages of sandstone and commonly maroon mudstone (e.g., Figure 6e), whereas the Glasgow member consists of gray, finely laminated mudstones (Figure 7b) that are commonly covered in enough dust to make laminations difficult to resolve (Figure 7c). As discussed above, west of Western butte and east of Central butte the contact (dotted line, Figure 10) represents a calculated fit anchored to four locations where the contact could be confidently placed.

5.5. Glasgow Member—Stimson Formation Contact

Across the GT region, and beyond, the contact between members of the Murray formation (Mount Sharp group) and the Stimson formation (Siccar Point group) is easily identified, and mapped with confidence, because rocks of the Stimson formation (Figures 2, 7a, and 12b), which overlie the Greenheugh pediment surface (Figures 3, 4 and 10), are well indurated and form a meters-tall steep cliff in most places in GT. In addition, the large-scale surface texture of the Stimson formation (previously, the "mound-skirting unit" of Anderson & Bell, 2010) is clearly distinct from Mount Sharp group rocks, which aids in mapping on HiRISE images. The Stimson formation is interpreted as an aeolian deposit and rests unconformably above the Glasgow member (Banham et al., 2022).

5.6. Stratigraphic Dip

As the geologic map (Figure 10) shows, the stratigraphic units have an approximately NE/SW strike and cross elevation contours to some degree, indicating that the lithologic units have at least some dip component. Regardless of which model is used to quantify dip (e.g., Kite et al., 2013; Stein et al., 2020), the values are small, ranging from near zero to approximately four degrees. While that range of dip angles is minimal, the values may be useful in understanding how the crater-filling succession formed and evolved to the present landscape.

In Gale crater, Murray formation strata have experienced substantial diagenetic overprint from the hundreds of meters-to-millimeter scale, which impacts outcrop expression (Christian et al., 2022; Hughes, 2021), physical

10.1029/2022JE007408

features at local scale (e.g., De Toffoli et al., 2020; Kronyak et al., 2019; Sun et al., 2019), geochemistry (Bedford et al., 2019; Bristow et al., 2021; Fraeman et al., 2020; Frydenvang et al., 2020; L'Haridon et al., 2018, 2020; Thompson et al., 2022), and mineralogy (Rampe et al., 2020). Ground observations by Curiosity show that diagenetic features may effectively obscure or even completely destroy primary layering, which gives rise to mappable strataform (but not stratabound) lithologic packages defined primarily as diagenetic bodies (e.g., FIU, Figure 4). In various locations throughout GT, fracture sets and aeolian sculpting can obscure primary bedding and create prominent surfaces that can be misidentified as bedding.

Two geologic cross-sections (A-A') along the same trend line (150°/330°, Figure 10), perpendicular to unit strike, placed where contacts are confidently located, and that pass through Central butte, were constructed to constrain the maximum dip that would still preserve lithologic unit fidelity (Figure 11). In constructing these cross sections, the Knockfarril Hill member plays a critical role because this unit represents a major change in primary lithology (mudstone to sandstone) that is not observed to that extent in most of the subjacent stratigraphic units. Knockfarril Hill strata also provide essential stratigraphic linkage between VRR and GT.

The top cross section depicts the strata at 0° dip. Bedding dip calculations made by Stein et al. (2020) utilized bedding tracings from high-resolution outcrop images across a decimeter scale at multiple locations to indicate that dip angles are <3° with various dip directions. Such a conclusion would be consistent with virtually no dip to the strata. The thickness of the stratigraphic column for the MSL mission (Figure 2) is drawn under assumption of a 0° dip.

The lower cross section depicts the stratigraphic units in GT with a 2° dip. A NNW dip direction was selected because long baseline analysis (Kite et al., 2013, 2016) envision dips spreading away from the center of Mount Sharp as does the work of Stein et al. (2020). Within GT, the lower and upper contacts of Knockfarril Hill strata offer two places to define the maximum dip angle using the topography and stratigraphic unit exposure at VRR and Central butte (Figure 11). Unlike most other unit boundaries that separate different mudstone-dominated members, the Jura—Knockfarril Hill members contact is recognized by a significant break in lithology making its identification much less speculative. Projecting any more than a 2° dip would place basal cross-stratified rocks of the Knockfarril Hill member at the top of VRR, although that does not occur anywhere in the study area (see extended, pink-shaded projection of Knockfarril Hill member, Figure 11). Similarly, if Knockfarril Hill strata had a greater dip, they should be exposed south of Central butte. Although Curiosity did not directly verify that, projecting this scenario toward the Western butte region (Figures 3 and 10) would require similarly incompatible outcrop patterns.

From a broader perspective, exposures of the stratigraphic units within GT provide clues as to how sedimentary material filled Gale crater in this region. The correlation of the Jura and Knockfarril Hill members, with dip angles <2°, across the topographic change from VRR to GT indicates that the sedimentary fill has been deeply eroded during the development of the modern surface relief. Facies within the stratigraphic units examined in this study do not define the margins of specific depositional environments, indicating they were much more extensive at the time of deposition relative to what Curiosity has been able to document in detail. As a consequence, models for the filling of the crater and formation of the present geomorphology need to account for deposition considerably more extensive than present exposures as was recognized by Grotzinger et al. (2015). This conclusion contrasts with models showing the central mound largely forming in place and only minimally eroded post deposition (e.g., Kite et al., 2013). Furthermore, the interpreted depositional systems, particularly lacustrine environments of the Jura member, essentially record paleohorizontal at the time of deposition, such that the possible up-to 2° dip must have occurred after deposition and not as a primary depositional slope.

6. Relationship Between Stratigraphy and Topography

Remotely sensed data and imagery taken from orbital platforms enabled a significant amount of research on the geologic units comprising the sedimentary fill of Gale crater, which provided critical context for guiding the traverse Curiosity would take on the ground (e.g., Anderson & Bell, 2010; Bennett et al., 2022; Fraeman et al., 2013, 2016; Grotzinger & Milliken, 2012; Malin & Edgett, 2000; Milliken et al., 2010; Thomson et al., 2011). Important geomorphic features such as "unit 5" (Malin & Edgett, 2000, now Greenheugh pediment) and "hematite ridge" (Fraeman et al., 2013, now VRR) generated testable hypotheses about the kinds of lithologies and stratal orientations essential to erecting a stratigraphic framework for the basin fill.

Within the GT study area, differential erosion, principally via wind, reveals variability in rock resistance, such as the prominent VRR and Greenheugh pediment. As differential erosion proceeds, the resultant variability in surface topography leads to a hierarchy of topographic features that may not be uniquely tied to specific lithologic units. These and other effects illustrate the challenge of defining and interpreting mappable stratigraphic units, geomorphic units, and hybrid units that may result from multiple processes.

Ground observations made by Curiosity along the full length of the traverse have tested the extent to which orbital platform-based observations accurately document actual stratigraphic relationships. VRR (formerly "unit 2", Malin & Edgett, 2000; light-toned ridge, Anderson & Bell, 2010; hematite ridge, Fraeman et al., 2013) forms a prominent geomorphic feature, with its very steep southern edge that defines the boundary with GT (Figures 4, 5a, and 11). The VRR versus GT contrast is not only obvious from HiRISE images, but also from spectral data that suggest that ridge is enriched in hematite (Fraeman et al., 2013, 2016), whereas the adjacent GT area is enriched in phyllosilicates (Fraeman et al., 2016; Milliken et al., 2010). Observations from Curiosity show that on VRR, Jura member (Murray formation) strata are highly indurated but pass directly through the ridge into GT where they form a geomorphic valley and low-angled slope (Figure 11) that carries a strong phyllosilicate signature (e.g., Fraeman et al., 2016). Hematite-rich Jura member rocks on VRR represent the same stratigraphy as those of the clay-rich valley/slope. Without rover-based facies recognition and correlation, a completely erroneous assessment of the stratigraphy, bedding orientation, and geologic history would be the likely outcome.

Another example from GT where topography does not match stratigraphy is the legacy unit named the "FIU" (Figures 4 and 7a), which is distinctly different from adjacent mappable geomorphic units, and whose northern contact broadly parallels stratigraphic member contacts (e.g., Hughes, 2021). The FIU shows a distinct outcrop pattern of meters-scale, fracture-bound, slabs much more resistant to weathering than the lower relief, less well exposed rocks in the region of the Visionarium and GT trough (Figure 3). Despite these FIU features, which most likely result from diagenesis, the underlying primary stratigraphy does not change, nor does the FIU contact directly follow stratigraphy. The lithologic boundary between the Knockfarril Hill and Glasgow members occurs in elevation above the FIU contact (Figure 7a). Thus, the FIU likely marks a diagenetic boundary that loosely follows stratigraphy, but does not correspond to changes in depositional facies.

Given the essential nature of geologic mapping as a means to decipher the history of Mars and that most mapping will be done using remotely sensed data sets, including via artificial intelligence/machine-learning approaches (e.g., Balme, 2021) as that approach advances, several important findings have emerged related to the integration of ground- and orbiter-based data that may be applied to other places where only remotely sensed data is possible. First, contacts between texturally/geomorphologically/compositionally different units do not necessarily carry stratigraphic significance. Such contacts may be the result of diagenetic mineral additions that affect rock induration and thus trace discordant but stratiform bodies. The amount of small-to large-scale diagenetic features on VRR and in GT is substantial, indicating that mapping projects using only remotely sensed data sets should expect such complications and consider post-depositional alteration in developing geological hypotheses. Second, where possible, the three-dimensional geometry of contact relationships should be constructed along with geologic cross sections to test how different contact relationships would manifest and produce the most geologically sound results. Third, planar surfaces such as fracture systems may appear at multiple orientations and produce confounding relationships that obscure or even obliterate bedding. Not all horizontal or sub horizontal contacts between map units can be assumed to represent primary depositional surfaces. Working out potential orders of cross-cutting relationships may help to reveal different planar features. Fourth, there is great potential for much deeper understanding of a region by making different maps of the same area that utilize multiple types of data and map units with the assumption that apparent contacts denote different types of information (e.g., geology, geomorphology, geochemistry, spectral) rather than representing homogenization of different data into a single map. Regions with contiguous spectral reflectance detections are commonly inferred as discrete geologic units, especially when the spatial extent coincides with morphological features; the GT region demonstrates how mitigating factors such as dust cover can follow topography and expose or obscure bedrock signatures. Creating complementary maps could highlight the strengths of a particular data set while also keeping sources of uncertainty at the forefront. While this paper provides a cautionary note for geologic mapping for using only remotely sensed data, such datasets are invaluable for generating critical testable hypotheses, guiding ground-based campaigns, and for integration with other datasets. Furthermore, new ground-based studies merging high-resolution geomorphic and compositional data (e.g., Hughes, 2021, 2022), provide exciting opportunities to merge interpretations about the formation of surface features, composition, and stratigraphy.

7. Conclusions

Detailed ground-based study of the sedimentology and stratigraphy of rocks that comprise the GT region in Gale crater, Mars, permit the following conclusions:

1. Strata in GT and the directly adjacent VRR consist of distinct lithostratigraphic packages that are divided into formation and member-level informal stratigraphic units. The upper part of the Murray formation comprises the Pettegrove Point and Jura members, both dominated by mudstone, but with the Jura containing some thin sandstone interbeds. The base of the Jura member is defined by a distinct, meters-thick, maroon-and-orange alternating lithofacies termed the "Flodigarry facies" after the Flodigarry target. Profusely cross-stratified sandstone of the Knockfarril Hill member of the Carolyn Shoemaker formation overlies the Jura member along a sharp contact. Meter-scale interfingering of mudstone and sandstone characterizes the upper part of the Knockfarril Hill member, which then is succeeded by finely laminated mudstone of the Glasgow member. In GT, the Glasgow member is unconformably overlain by the Stimson formation, which is part of the Greenheugh pediment, and forms the southern margin of the study area.
2. Two lithofacies in the stratigraphic succession, the Flodigarry facies and the basal cross-bedded Knockfarril Hill member, provide distinctions that allow for potential correlation between VRR and GT. The Flodigarry facies was defined on the north side of VRR, but then appears again at about the same elevation in GT, in the valley that runs parallel to VRR. This indicates that this facies crosses the geomorphic divide that separates VRR and GT. Furthermore, the base of the Knockfarril member similarly spans from the southern margin of VRR to widespread occurrences across the entire GT region. Despite being exposed as part of quite different geomorphic (and spectroscopic and thermophysical) regions, the strata can be confidently correlated, indicating they form part of a continuous succession.
3. Mudstone and cross-bedded sandstone form the main lithologies of the rocks exposed in GT. Mudstone deposits typically consist of millimeter-scale laminations, interpreted to be the deposits of lake deposition. The cross-bedded sandstones (basal Knockfarril Hill member) are consistent with having formed as accumulations of stacked fluvial bars in a braided stream environment. Because the sandstones correlate throughout GT, we conclude that they represent a widespread depositional unit that signifies a considerable change in environment and the base of a new depositional episode.
4. Lithostratigraphic units are distinct enough that their contacts can be transferred to a HiRISE base image, making a geologic map. Contacts between units are defined using characteristics in the vicinity of the rover, including lithologic changes and outcrop expression. Most units were crossed multiple times within the VRR and GT regions, adding substantial confidence to the mapping. Away from the rover traverse, contacts were extended using images taken from Curiosity and outcrop patterns unique to the contact. A geologic cross section drawn perpendicular to the NE strike of the units permits that the strata to dip no more than 2° NW.
5. This study illustrates the complexity of interpreting stratigraphy based on geomorphology alone. In the case of VRR and GT, distinct stratigraphic units cross-cut major geomorphic boundaries, suggesting that caution is warranted when linking geomorphology and primary depositional environments or conditions.

Data Availability Statement

All data are available via the Planetary Data System (PDS; https://pds-geosciences.wustl.edu/dataserv/doi.htm). The PDS contains all Mastcam (Malin, 2013), MAHLI (Edgett, 2013), and ChemCam RMI (Weins, 2013) images/data shown or utilized in this research. Alpha Particle X-Ray Spectrometer (APXS) data (Gellert, 2013) is also available on the PDS. The geologic map is available in open access format (Fedo et al., 2022).

Acknowledgments

Some of the research was carried out at the Jet Propulsion Laboratory, California Institute of Technology, under a contract with the National Aeronautics and Space Administration (NASA). CMF, LAE, KMS, DMR, AAF, RMW acknowledge funding by the NASA MSL Participating Scientist Program (NNH15ZDA001 N). GC was supported by the French space agency CNES under convention CNES 180027. Steven G. Banham and Sanjeev Gupta acknowledge funding from the UK Space Agency (UKSA) (Grant numbers: ST/W002280/1; ST/N000579/1; ST/S001492/1; ST/S001506/1; ST/T001755/1). CMF thanks S. Gwizd for discussions about the stratigraphy and paleoenvironments of the Murray formation. We thank the reviewers for constructive comments that improved the manuscript.

References

Anderson, R. B., & Bell, J. F., III. (2010). Geologic mapping and characterization of Gale crater and implications for its potential as a Mars Science Laboratory landing site. *International Journal of Mars Science and Exploration*, *5*, 76–128. https://doi.org/10.1555/mars.2010.0004

Balme, M. (2021). *Team-based, bespoke, and machine learning: Different ways to map Mars from remote sensing data: William Smith virtual Meeting, geological mapping - of our world and others*. The Geological Society of London.

Banham, S. G., Gupta, S., Rubin, D. M., Bedford, C. C., Edgar, L., Bryk, A., et al. (2022). Evidence for seasonal and long-duration wind fluctuations in an ancient aeolian dune field: Reconstruction of the Hesperian Stimson formation at the Greenheugh pediment, Gale crater, Mars. *Journal of Geophysical Research – Planets*. https://doi.org/10.1029/2021JE007023

Banham, S. G., Gupta, S., Rubin, D. M., Edgett, K. S., Barnes, R., Van Beek, J., et al. (2021). A rock record of complex Aeolian bedforms in a Hesperian Desert landscape: The Stimson formation as exposed in the Murray Buttes, Gale crater, Mars. *Journal of Geophysical Research: Planets*, *126*(4). https://doi.org/10.1029/2020JE006554

Banham, S. G., Gupta, S., Rubin, D. M., Watkins, J. A., Sumner, D. Y., Edgett, K. S., et al. (2018). Ancient Martian aeolian processes and palaeomorphology reconstructed from the Stimson formation on the lower slope of Aeolis Mons, Gale crater, Mars. *Sedimentology*, *65*(4), 993–1042. https://doi.org/10.1111/sed.12469

Bedford, C. C., Bridges, J. C., Schwenzer, S. P., Weins, R. C., Rampe, E. B., & Gasda, P. J. (2019). Alteration trends and geochemical source region characteristics preserved in the fluviolacustrine sedimentary record of Gale crater, Mars. *Journal of Geophysical Research: Planets*, *137*, 234–266. https://doi.org/10.1016/j.gca.2018.11.031

Bennett, K. A., Fox, V., Bryk, A., Dietrich, W., Fedo, C., Edgar, L., et al. (2022). The Curiosity rover's exploration of Glen Torridon, Gale crater, Mars: An overview of the campaign and scientific results. *Journal of Geophysical Research: Planets*. https://doi.org/10.1029/2022JE007185

Boggs, S., Jr. (2012). *Principles of sedimentology and stratigraphy* (5th ed., p. 585). Prentice Hall.

Bristow, T. F., Grotzinger, J. P., Rampe, E. B., Cuadros, J., Chipera, S. J., Downs, G. W., et al. (2021). Brine-driven destruction of clay minerals in Gale crater, Mar. *Science*, *373*(6551), 198–204. https://doi.org/10.3390/min11080847

Bryk, A. B., Deitrich, W. E., Lamb, M. P., Grotzinger, J. P., Vasavada, A. R., Stack, K. M., et al. (2019). What was the original extent of the Greenheugh pediment and Gediz Vallis. *Ninth International Conference on Mars*. Abstract 6296.

Calef, F. J., III, Abarca, H. E., Soliman, T., Abercrombie, S. P., & Powell, M. W. (2019). *Multi-mission geographic information system: An open-source solution for planetary science operations*. 4th Planetary Data Workshop. Abstract 7071.

Calef, F. J., III, Gengl, H. E., Soliman, T., Abercrombie, S. P., & Powell, M. W. (2017). MMGIS: A multi-mission geographic information system for in situ Mars operations. In *the 48th lunar and planetary science conference*. Abstract 2541.

Calef, F. J., III, & Parker, T. (2016). *MSL Gale merged orthophoto mosaic. PDS Annex*. U.S. Geological Survey. Retrieved from http://bit.ly/MSL_Basemap

Caravaca, G., Mangold, N., Dehouk, E., Schieber, J., Zaugg, L., Bryk, A. B., et al. (2022). From lake to river: Documenting an environmental transition across the Jura/Knockfarril Hill members boundary in the Glen Torridon region of Gale crater (Mars). *Journal of Geophysical Research: Planets*. https://doi.org/10.1029/2021JE007093

Christian, J. R., Arvidson, R. E., O'Sullivan, J. A., Vasavada, A. R., & Weitz, C. M. (2022). CRISM-based high spatial resolution thermal inertia mapping along Curiosity's traverses in Gale crater. *Journal of Geophysical Research – Planets*, *127*(5). https://doi.org/10.1029/2021JE007076

Dehouck, E., Cousin, A., Mangold, N., Frydenvang, J., Gasnault, O., Forni, O., et al. (2022). Bedrock geochemistry and alteration history of the clay-bearing Glen Torridon region of Gale crater, Mars. *Journal of Geophysical Research: Planets*, *127*. https://doi.org/10.1029/2021JE007103

De Toffoli, B., Mangold, N., Massironi, M., Zanella, A., Pozzobon, R., Le Mouélic, S., et al. (2020). Structural analysis of sulfate vein networks in Gale crater, Mars. *Journal of Structural Geology*, *137*, 104083. https://doi.org/10.1016/j.jsg.2020.104083

Edgar, L. A., Fedo, C. M., Gupta, S., Banham, S. G., Fraeman, A. A., Grotzinger, J. P., et al. (2020). A lacustrine paleoenvironment recorded at Vera Rubin Ridge, Gale crater: Overview of the sedimentology and stratigraphy observed by the Mars Science Laboratory Curiosity. *Journal of Geophysical Research: Planets*, *125*(3). https://doi.org/10.1029/2019je006307

Edgett, K. S. (2013). MSL Mars Hand Lens Imager 4 RDR Image V1.0. [Data Set]. NASA Planetary Data System. https://doi.org/10.17189/1520292

Edgett, K. S., Yingst, R. A., Ravine, M. A., Caplinger, M. A., Maki, J. N., Ghaemi, F. T., et al. (2012). Curiosity's Mars hand lens imager (MAHLI) investigation. *Space Science Reviews*, *170*(1), 259–317. https://doi.org/10.1007/s11214-012-9910-4

Fedo, C. M., Bryk, A. B., Edgar, L. A., Bennett, K. A., Fox, V. K., Dietrich, W. E., et al. (2022). *Geologic map of the Glen Torridon region*. Gale crater, Mars. https://doi.org/10.5281/zenodo.7041712

Fox, V. K., Bennett, K. A., Vasavada, A. R., Stack, K. M., & Ehlmann, B. L. (2018). The clay-bearing unit of the Mount Sharp, Gale crater, I: Orbital perspective and initial results. In *49th lunar planetary science conference*. Abstract 1728.

Fraeman, A. A., Arvidson, R. E., Catalano, J. G., Grotzinger, J. P., Morris, R. V., Murchie, S. L., et al. (2013). A hematite-bearing layer in Gale Crater, Mars: Mapping and implications for past aqueous conditions. *Geology*, *41*(10), 1103–1106. https://doi.org/10.1130/G34613.1

Fraeman, A. A., Edgar, L. A., Rampe, E. B., Thompson, L. M., Frydenvang, J., Fedo, C. M., et al. (2020). Evidence for a diagenetic origin of Vera Rubin ridge, Gale crater, Mars: Summary and synthesis of Curiosity's exploration campaign. *Journal of Geophysical Research: Planets*, *125*(12). https://doi.org/10.1029/2020JE006527

Fraeman, A. A., Ehlmann, B. L., Arvidson, R. E., Edwards, C. S., Grotzinger, J. P., Milliken, R. E., et al. (2016). The stratigraphy and evolution of lower Mount Sharp from spectral, morphological, and thermophysical orbital data sets. *Journal of Geophysical Research: Planets*, *121*(9), 1713–1736. https://doi.org/10.1002/2016JE005095

Frydenvang, J., Mangold, N., Wiens, R. C., Fraeman, A. A., Edgar, L. A., Fedo, C. M., et al. (2020). The chemostratigraphy of the Murray formation and role of diagenesis at Vera Rubin ridge in Gale crater, Mars, as observed by the ChemCam instrument. *Journal of Geophysical Research: Planets*, *125*(9). https://doi.org/10.1029/2019JE006320

Gellert, R. (2013). MSL Mars alpha particle X-ray spectrometer 4/5 RDR V1.0. [Data Set]. NASA Planetary Data System. https://doi.org/10.17189/1519440

Grotzinger, J. P., Crisp, J., Vasavada, A. R., Anderson, R. C., Baker, C. J., Barry, R., et al. (2012). Mars Science Laboratory Mission and Science Investigation. *Space Science Reviews*, *170*(1–4), 5–56. https://doi.org/10.1007/s11214-012-9892-2

Grotzinger, J. P., Gupta, S., Malin, M. C., Rubin, D. M., Schieber, J., Siebach, K., et al. (2015). Deposition, exhumation, and paleoclimate of an ancient lake deposit, Gale crater, Mars. *Science*, *350*(6257), aac7575. https://doi.org/10.1126/science.aac.7575

Grotzinger, J. P., & Milliken, R. (2012). The sedimentary rock record of Mars: Distribution, origins, and global stratigraphy. *Society for Sedimentary Geology Special Publication: Sedimentary Geology of Mars*, *102*, 1–48. https://doi.org/10.2110/pec.12.102.0001

Gwizd, S., Fedo, C., Grotzinger, J., Banham, S., Rivera-Hernandez, F., Stack, K. M., et al. (2022). Sedimentological and geochemical perspectives on a marginal lake environment recorded in the Hartmann's Valley and Karasburg members of the Murray formation, Gale crater, Mars. *Journal of Geophysical Research: Planets*, *127*(8). https://doi.org/10.1029/2022JE007280

He, L., Arvidson, R. E., O'Sullivan, J. A., Morris, R. V., Hughes, M. N., & Powell, K. E. (2022). Surface kinetic temperatures and nontronite single scattering albedo spectra from Mars Reconnaissance Orbiter CRISM Hyperspectral Imaging data over Glen Torridon, Gale crater, Mars. *Journal of Geophysical Research: Planets*. https://doi.org/10.1029/2021JE007092

Hughes, M. N. (2021). *Landscape evolution at Endeavour and Gale Craters on Mars, and how terrain characteristics correlate with mineralogy on lower Mount Sharp, Gale crater* (Vol. 2428). Washington University in St. Louis Arts & Sciences Electronic Theses and Dissertations. https://doi.org/10.7936/C6SE-5895

Hughes, M. N. (2022). Geomorphic map of Glen Torridon in Gale crater, Mars. In *Digital research materials (data & supplemental files)* (Vol. 95). https://doi.org/10.7936/0cyw-3n10

Kah, L. C., Stack, K., Eigenbrode, J., Yingst, R. A., & Edgett, K. (2018). Implications of syndepositional calcium sulfate precipitation in Gale crater, Mars. *Terra Nova*, *30*(6), 431–439. https://doi.org/10.1111/ter.12359

Kite, E. S., Lewis, K. W., Lamb, M. P., Newman, C. E., & Richardson, M. I. (2013). Growth and form of the mound in Gale crater, Mars: Slope wind enhanced erosion and transport. *Geology*, *41*(5), 543–546. https://doi.org/10.1130/G33909.1

Kite, E. S., Sneed, J., Mayer, D. P., Lewis, K. W., Michaels, T. I., Hore, A., & Rafkin, S. C. R. (2016). Evolution of major sedimentary mounds on Mars: Buildup via anticompressional stacking modulated by climate change. *Journal of Geophysical Research: Planets*, *121*(11), 2282–2324. https://doi.org/10.1002/2016JE005135

Kronyak, R. E., Kah, L. C., Edgett, K. S., VanBommel, S. J., Thompson, L. M., Wiens, R. C., et al. (2019). Mineral-filled fractures as indicators of multigenerational fluid flow in the Pahrump Hills member of the Murray formation, Gale crater, Mars. *Earth and Space Science*, *6*(2), 238–265. https://doi.org/10.1029/2018EA000482

L'Haridon, J., Mangold, N., Fraeman, A. A., Johnson, J. R., Cousin, A., Rapin, W., et al. (2020). Iron mobility during diagenesis at Vera Rubin ridge, Gale crater, Mars. *Journal of Geophysical Research: Planets*, *125*(11). https://doi.org/10.1029/2019JE006299

Le Mouélic, S., Gasnault, O., Herkenhoff, K. E., Bridges, N. T., Langevin, Y., Mangold, N., et al. (2015). The ChemCam remote micro-imager at Gale crater: Review of the first year of operations on Mars. *Icarus*, *249*, 93–107. https://doi.org/10.1016/j.icarus.2014.05.030

L'Haridon, J., Mangold, N., Meslin, P.-Y., Johnson, J. R., Rapin, W., Forni, O., et al. (2018). Chemical variability in mineralized veins observed by ChemCam on the lower slopes of Mount Sharp in Gale crater, Mars. *Icarus*, *311*, 69–86. https://doi.org/10.1016/j.icarus.2018.01.028

Long, D. G. F. (2011). Architecture and depositional style of fluvial systems before land plants: A comparison of Precambrian, early Paleozoic modern river deposits. In S. Davidson, S. Leleu, & C. P. North (Eds.), *From river to rock record: The preservation of fluvial sediments and their subsequent interpretation*, (Vol. 97, pp. 37–61). SEPM, Special Publication.

Maki, J. (2018). MSL Mars Navigation Camera 5 RDR V2.0. [Data Set]. NASA Planetary Data System. https://doi.org/10.17189/1519572

Maki, J., Thiessen, D., Pourangi, A., Kobzeff, P., Litwin, T., Scherr, L., et al. (2012). The Mars Science Laboratory Engineering cameras. *Space Science Reviews*, *170*(1–4), 77–93. https://doi.org/10.1007/s11214-012-9882-4

Malin, M. C. (2013). MSL MARS Mast Camera 2 EDR ZSTACK V1.0. [Data set]. NASA Planetary Data System. https://doi.org/10.17189/1520215

Malin, M. C., & Edgett, K. S. (2000). Sedimentary rocks of early Mars. *Science*, *290*(5498), 1927–1937. https://doi.org/10.1126/science.290.5498.1927

Malin, M. C., Ravine, M. A., Caplinger, M. A., Ghaemi, F. T., Schaffner, J. A., Maki, J. N., et al. (2017). The Mars Science Laboratory (MSL) Mast cameras and Descent imager: Investigation and instrument descriptions. *Earth and Space Science*, *4*(8), 506–539. https://doi.org/10.1002/2016EA000252

McAdam, A. C., Sutter, B., Archer, P. D., Franz, H. B., Wong, G. M., Lewis, J. M. T., et al. (2022). Evolved gas analyses of sedimentary rocks from the Glen Torridon clay-bearing Unit, Gale crater, Mars: Results from the Mars Science Laboratory sample Analysis at Mars instrument suite. *Journal of Geophysical Research: Planets*. https://doi.org/10.1029/2022JE007179

McEwen, A. (2005). MRO Mars High Resolution Image Science Experiment EDR V1.0. [Data set]. NASA Planetary Data System. https://doi.org/10.17189/1520179

McEwen, A. S., Eliason, E. M., Bergstrom, J. W., Bridges, N. T., Hansen, C. J., Delamere, W. A., et al. (2007). Mars Reconnaissance Orbiter's High Resolution Imaging Science Experiment (HiRISE). *Journal of Geophysical Research*, *112*(E5), E05S02. https://doi.org/10.1029/2005JE002605

Milliken, R. E., Grotzinger, J. P., & Thomson, B. J. (2010). Paleoclimate of Mars as captured by the stratigraphic record in Gale Crater. *Geophysical Research Letters*, *37*(4). https://doi.org/10.1029/2009GL041870

Muhlbauer, J. G., Fedo, C. M., & Moersch, J. E. (2020). Architecture of a distal pre-vegetation braidplain: Cambrian middle member of the Wood Canyon Formation, southern Marble Mountains, California, USA. *Sedimentology*, *67*(2), 1084–1113. https://doi.org/10.1111/sed.12677

O'Connell-Cooper, C. D., Thompson, L. M., Spray, J. G., Berger, J. A., Gellert, R., McCraig, M., et al. (2022). Statistical analysis of APXS-derived chemistry of the clay-bearing Glen Torridon region and Mount Sharp group, Gale crater, Mars. *Journal of Geophysical Research: Planets*. https://doi.org/10.1029/2021JE007177

Rampe, E. B., Blake, D. F., Bristow, T. F., Ming, D. W., Vaniman, D. T., Morris, R. V., et al. (2020). Mineralogy and geochemistry of sedimentary rocks and eolian sediments in Gale crater, Mars: A review after six Earth years of exploration with Curiosity. *Geochemistry*, *80*(2), 125605. https://doi.org/10.1016/j.chemer.2020.125605

Schieber, J., Bish, D., Coleman, M., Reed, M., Hausrath, E., Cosgrove, J., et al. (2017). Encounters with an unearthly mudstone: Understanding the first mudstone found on Mars. *Sedimentology*, *64*(2), 311–358. https://doi.org/10.1111/sed.12318

Stack, K. M., Dietrich, W. E., Lamb, M. P., Sullivan, R. L., Christian, J. R., Newman, C. E., et al. (2022). Orbital and in-situ investigation of periodic bedrock ridges in Glen Torridon, Gale crater, Mars. *Journal of Geophysical Research: Planets*, *127*(6). https://doi.org/10.1029/2021JE007096

Stack, K. M., Grotzinger, J. P., Lamb, M. P., Gupta, S., Rubin, D. M., Kah, L. C., et al. (2019). Evidence for plunging river plume deposits in the Pahrump Hills member of the Murray formation, Gale crater, Mars. *Sedimentology*, *66*(5), 1768–1802. https://doi.org/10.1111/sed.12558

Stein, N. T., Quinn, D. P., Grotzinger, J. P., Fedo, C., Ehlmann, B. L., Stack, K. M., et al. (2020). Regional structural orientation of the Mount Sharp group revealed by in situ dip measurements and stratigraphic correlations on the Vera Rubin ridge. *Journal of Geophysical Research: Planets*, *125*(5). https://doi.org/10.1029/2019JE006298

Sun, V. Z., Stack, K. M., Kah, L. C., Thompson, L., Fischer, W., Williams, A., et al. (2019). Late-stage concretions in the Murray formation, Gale crater, Mars. *Icarus*, *321*, 866–890. https://doi.org/10.1016/j.icarus.2018.12.030

Thompson, L. M., Spray, J. G., O'Connell-Cooper, C., Berger, J. A., Yen, A., Boyd, N., et al. (2022). Alteration at the base of the Siccar Point unconformity and further 1 evidence for an alkaline provenance at Gale crater: Exploration of the Mount Sharp group, Greenheugh pediment cap rock contact with APXS. *Journal of Geophysical Research: Planets*. https://doi.org/10.1029/2021JE007178

Thomson, B. J., Bridges, N. T., Milliken, R., Baldridge, A., Hook, S. J., Crowley, J. K., et al. (2011). Constraints on the origin and evolution of the layered mound in Gale crater, Mars using Mars Reconnaissance Orbiter data. *Icarus*, *214*(2), 413–432. https://doi.org/10.1016/j.icarus.2011.05.002

Thorpe, M. T., Bristow, T. F., Rampe, E. B., Tosca, N. J., Grotzinger, J. P., Bennett, K. A., et al. (2022). Mars Science Laboratory CheMin data from the Glen Torridon region and the significance of lake-groundwater interactions in interpreting mineralogy and sedimentary history. *Journal of Geophysical Research: Planets*. https://doi.org/10.1029/2021JE007099

Weins, R. C. (2013). MSL Mars ChemCam Remote Micro-Imager Camera 5 RDR V1.0. [Data Set]. NASA Planetary Data System. https://doi.org/10.17189/1519494

Wiens, R. C., Maurice, S., Barraclough, B., Saccoccio, M., Barkley, W. C., Bell, J. F., et al. (2012). The ChemCam instrument suite on the Mars Science Laboratory (MSL) rover: Body unit and combined system tests. *Space Science Reviews*, *170*(1), 167–227. https://doi.org/10.1007/s11214-012-9902-4

Williams, R. M. E., Grotzinger, J. P., Dietrich, W. E., Gupta, S., Sumner, D. Y., Wiens, R. C., et al. (2013). Martian fluvial conglomerates at Gale crater. *Science*, *340*(6136), 1068–1072. https://doi.org/10.1126/science.1237317